The effects of sodium butyrate on *Hox* gene expression in human colorectal adenocarcinoma cell line, HT29.

by
Lucy D. Conaty
June 2013

Director of Thesis: Jean-Luc Scemama, Ph.D.
Major Department: Biology

Hox genes are a subgroup of the large family of homeobox containing genes, known to pattern anterior/posterior and proximal/distal axes during embryonic development. More recently *Hox* gene research has focused on the role of these genes during carcinogenesis. We studied the pattern of *Hox* gene expression in a human colorectal adenocarcinoma cell line, HT29, in response to treatment with a histone deacetylase inhibitor, sodium butyrate. Sodium butyrate treatment has been previously described to differentiate HT29 cells. The cells acquire differentiated characteristics after a seven-day treatment period with 5 mM sodium butyrate. These features include increased microvilli concentrations, tight junctions, and the formation of apical and basolateral domains. Our research aimed to study the role of *Hox* genes in colorectal cancer by analyzing their expression in both proliferative and growth-inhibited HT29 cells. The first phase of our research was to determine the pattern of expression for all 39 characterized human *Hox* genes using RT-PCR in order to select genes of interest that are differentially between proliferating and differentiated HT29 cells. The second was to verify the differential expression of these genes with qRT-PCR and Western blot. It was observed that most genes of cluster D were expressed in untreated but not treated HT29 cells. More specifically, D8 and D9 were the only two genes of this cluster with a differential pattern of expression than the other genes of their paralog groups. We hypothesized that D8 and D9 are

responsible for maintaining the proliferative, undifferentiated state of the HT29 cells. Using qRT-PCR analysis, D8 was shown to be up-regulated in untreated HT29 cells in comparison to treated HT29 when normalized to housekeeping genes. However, D9 was shown to be down-regulated in untreated HT29 in comparison to treated HT29 when normalized to housekeeping genes. The Western blot for *Hox* D9 reflected the findings of RT-PCR but not qRT-PCR. Protein expression was present in untreated HT29 cell lysates, but not the sodium butyrate treated lysates. D8 showed no protein expression in either untreated or treated cell lysates. The effects of sodium butyrate treatment on HT29 cell proliferation and differentiation was assessed using growth curves and ultrastructural analysis by transmission electron microscopy. It was observed that when cells are seeded at a low density (9.6×10^4) and recorded for seven days, sodium butyrate treatment effectively inhibited cellular proliferation. Electron micrographs showed that NaBT treated HT29 cells exhibited potential apical domains, increased concentrations of microvilli, tight junctions and approximately double the number of desmosomes at intercellular junctions. In addition, some of the treated cells exhibited the formation of mucin granules, specific to the phenotype of epithelial goblet cells.

The effects of sodium butyrate on *Hox* gene expression in human colorectal adenocarcinoma cell line, HT29.

A Thesis

Presented To the Faculty of the Department of Biology

East Carolina University

In Partial Fulfillment of the Requirements for the Degree

Master of Science, Molecular Biology and Biotechnology

by

Lucy D. Conaty

June 2013

The effects of sodium butyrate on *Hox* gene expression in human colorectal carcinoma cell line, HT29.

by

Lucy D. Conaty

APPROVED BY:

DIRECTOR OF
THESIS: _____
Jean-Luc Scemama, PhD

COMMITTEE MEMBER: _____
Margit Schmidt, PhD

COMMITTEE MEMBER: _____
Tim Christensen, PhD

COMMITTEE MEMBER: _____
Nicholas Polakowski, PhD

CHAIR OF THE DEPARTMENT
OF BIOLOGY: _____
Jeff McKinnon, PhD

DEAN OF THE
GRADUATE SCHOOL: _____
Paul Gemperline, PhD

ACKNOWLEDGEMENTS

First and foremost, I would like to thank my family. Mom and Dad, although I don't feel as if I can put my gratitude into words, thank you for allowing me to further my education; tirelessly encouraging me; and being temporary grand-dog guardians to Molson. My siblings, Helen and Peter, thank you for always listening to my stories and entertaining me when I needed a distraction (or ten). To both sets of my loving grandparents, thank you for all of your continuous words of encouragement. I would also like to thank my amazing boyfriend, Greg, for always being there for support and loving me. Furthermore, thanks to my sweet Molson for being the best little sidekick and guard dog a girl could ask for. I couldn't have done this without any of you.

Many thanks to my advisors Dr. Jean-Luc Scemama and Dr. Margit Schmidt for all of your contributions, guidance, and hospitality; I greatly appreciate everything you have both done for me. In addition to my advisors, a special thank you to the other members of my thesis committee: Dr. Tim Christensen and Dr. Nicholas Polakowski.

Lastly, I would like to acknowledge my lab mates Melissa Harkins, Kelli Shortt, and Dan White. Thanks for the numerous food and coffee runs, helping to maintain some level of sanity, continuous troubleshooting, ridiculous conversation, and so on. On most days, y'all helped make three years a little more bearable.

TABLE OF CONTENTS

LIST OF TABLES

LIST OF FIGURES

LIST OF ABBREVIATIONS

ACTB: β-Actin
APS: Ammonium Persulfate
ATCC: American Type Culture Collection
Avg: Average
B2M: β-2 Microglobulin
bp: Basepairs
cDNA: Complementary Deoxyribonucleic Acid
DMEM/F12: Dulbecco's Modified Eagle Medium/Ham's F12 Medium (1:1)
dNTPs: Deoxyribonucleotides
DNA: Deoxyribonucleic acids
DTT: Dithiothreitol
E: Efficiency
EDTA: Ethylenediamminetetraacetic Acid
FAP: Familial Adenomatous Polyposis
FBS: Fetal Bovine Serum
GAPDH: Glyceraldehyde-3-Phosphate Dehydrogenase
gDNA: Genomic DNA
GOI: Gene of Interest
H_2O: Water
HCl: Hydrochloric Acid
HDAC: Histone Deacetylase
HEPES: 4-(2-Hydroxyethyl)piperazine-1-ethanesulfonic acid
HKPG: Housekeeping
HRP: Horseradish Peroxidase
IgG: Immunoglobulin G
kDa: kiloDaltons
M: Molar
mAmps: milliAmperes
$MgCl_2$:
mL: Milliliter
mM: Millimolar
NaBT: Sodium Butyrate
NaCl: Sodium Chloride
NaF: Sodium Fluoride
nm: Nanometers
Oligo(dT): Deoxythymidylic acid residue primer sequence
OsO_4: Osmium Tetroxide
PBS: Phosphate Buffer Saline
PCI: 25:24:1 Phenol Chloroform Isoamyl Alcohol
PenStrep: Penicillin Steptomycin
PMSF: Phenolmethylsulfonyl Fluoride
PVDF: Polyvinylidene Difluoride Membrane
qRT-PCR/qPCR: Quantitative Real-time Polymerase Chain Reaction
RFU: Relative Fluorescence Unit
RNA: Ribonucleic Acid
RPLP0: Human Acidic Ribosomal Protein 0
RPL13a: Ribosomal Protein L13a
RT: Reverse Transcriptase
RT-PCR: Reverse Transcription Polymerase Chain Reaction

SDS: Sodium Dodecyl Sulfate
SDS-PAGE: Sodium Dodecyl Sulfate Polyacrylamide Gel Electrophoresis
T: Treated
TALE: 3-Amino Acid Loop Extension Family
TBP: TATA Binding Protein
TBS: Tris Buffered Saline
TBST: Tris Buffered Saline with Tween 20
TEMED: Tetramethylethylenediamine
TFRC: Transferrin Receptor C
UT: Untreated
V: Volts
Vol: Volume
VIL1: Villin
λ = wavelength
µL: Microliter
µm: Micrometer

Chapter 1: Introduction

Each year in the United States, there are over 100,000 new diagnosed cases of colorectal cancer; more than 50,000 of these cases result in death. The majority of these diagnosed colorectal cancers begin as adenocarcinomas. Among the advancing treatment options, targeted cancer therapies have been heavily studied due to their level of effectiveness and less harmful nature. [CDC 2012] This targeted cancer therapy, or gene therapy, focuses on ways to manipulate genes that are responsible for promoting tumor growth and metastases. The heightened interest in and need for viable targets for gene therapy influenced the direction of this project.

1.1.1: *Hox* Genes: Homeobox-containing Genes

Hox genes are a subgroup of the large family of homeobox-containing genes, originally discovered in the common fruit fly, *Drosophila melanogaster* [Grier 2005, Shah 2010]. In *Drosophila*, these genes control the body plan during embryonic development. Due to this property, they were named homeotic genes [Freschi 2005]. The developmental roles of these genes were determined by mutations that arose as phenotypical changes: i.e. legs replaced by antennae [Shah 2010].

The homeobox is a sequence of DNA approximately 180 base pairs in length, which encodes a protein domain known as the homeodomain. This domain, located within exon 2, encodes a DNA binding motif and is relatively well conserved among *Hox* genes. Hox proteins can function to directly drive transcription of targeted genes or interact with members of the 3-amino acid loop extension family of cofactors (TALE). [Shah 2010]

While *Hox* genes have been well described for their role in embryonic development, it is now clear that they are also important in post-embryonic maintenance of the organism. In addition, there has been a suggested potential role of homeodomain-containing proteins in neoplasia of cancer lesions. These roles are attributed to viral integrations and translocations within the genes, in part causing the onset of oncogenesis. Some of these genes are members of the HOMC/*Hox* family while others are members of the other characterized homeotic gene families. [Chariot 1996]

1.1.2: *Hox* Genes: Evolutionary History

Homeobox-containing genes are found in all bilateral organisms. They are commonly described as evolutionarily conserved transcription factors that function to pattern the development of embryos and participate in tissue differentiation.

Humans have over 200 homeobox genes dispersed throughout the genome. [Abate-Shen 2002, Freschi 2005] However, only 39 of these 200+ genes belong to the *Hox* gene family. Mammalian *Hox* genes are organized into four clusters—A, B, C and D—located on different chromosomes (7, 17, 12 and 2, respectively). The number of clusters varies amongst organisms and the complexity of their anatomy. [Shah 2010] Although the number of clusters/complexity corollary does not necessarily dictate that more complex

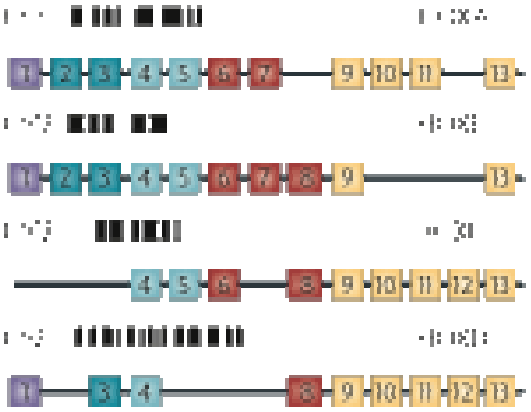

Figure 1. Hox gene family diagram, showing the clusters on their respective chromosomes depicting paralogs in their spatial colinear alignment. The colors represent dominance, purple being most dominant and yellow being the least. Reprinted by permission from Macmillan Publishers Ltd: Nature Reviews Cancer (Shah 2010), copyright 2010.

organisms have a greater number of clusters. Each of these four complexes of clusters spans approximately 200 kilobases and contains between 9 to 11 genes each [Zeltser1996]. These four complexes arose by two rounds of genome duplication. Therefore, *Hox* genes that are located at the same position in different clusters (thus separate chromosomes) are called paralogs. These paralogs are a division of the homologs, or genes sharing a common origin. Due to common ancestry, the paralogous genes may have similar, overlapping functions or a new function due to lack of selective pressure on one or more copies of the duplicated gene. That is to say that genes on different chromosomes that are located in the same position have more similar patterns of expression and share more sequence similarities than genes located along the same chromosome in varying positions [Greer 2000]. In vertebrates, there are 13 paralog groups. These paralogs are numbered along a chromosomal axis, with 1 being the most 3' and 13 being the most 5'. The expression of these genes along the anterior-posterior body axis corresponds to their position along the 3' to 5' cluster. The 3' genes are expressed more anteriorly than those of the 5' region. [Shah 2010] This property is described as spatiotemporal colinearity [Grier 2005].

Interestingly, between humans and mice, most paralogous subsets have been maintained in both organisms [Zeltser 1996]. A significant number of murine studies have been conducted in order to determine the roles of these *Hox* genes *in vivo*. For example, to determine overlapping function of paralogous genes, a group of researchers [Greer 2000] study paralog group 3 to determine the biological function of these related genes. They discovered that genes *Hoxa*3, *b*3 and *d*3 in mice share nearly identical patterns of expression and approximately 50% similarity of protein-coding sequences. In contrast, they determined that knocking out either one of *Hoxa*3 or *d*3 resulted in no overlapping phenotypes. These data suggest that the genes may

have acquired different functions through interaction with different partner proteins. [Greer 2000]

1.2.1: Developmental Roles: *Hox* Genes

Hox genes serve as a template of development along the anterior-posterior and proximal-distal body axes of bilateral organisms. During embryogenesis, *Hox* gene expression pattern reflects their roles in segmentation, location along the chromosome and within a cluster, and the fate of varying tissue and cell types [Abate-Shen 2002]. In balanced expression of these genes, *Hox* genes also drive the development of organs [Shah 2010].

1.2.2: Developmental Roles: *Hox* Paralogs 8 and 9

Hox paralog groups 8 and 9 contain seven genes: A9, B8, B9, C8, C9, D8 and D9. These genes are expressed more posteriorly, with their locations closer to the 5' end of the chromosome [Figure 1]. For example, in developing mice, *Hox* genes a9, b9 and d9 control the development of mammary glands and ducts in response to pregnancy. [Chen 1999] In the development of chick limbs, it has also been observed that 5'-most genes of *Hox*a and *Hox*d clusters are expressed in the wrist, ankles and digits. The expression of these genes were localized to developmental regions of the forelimb and proximal limb, including the humerus, femur, fibula/tibula or radius/ulna. [Grier 2005]

1.3.1: Post-embryonic and Oncogenic Roles: Hox Genes

While *Hox* genes have been extensively studied during embryonic development, they are also expressed in various adult tissues [Boudreau 1997, Freschi 2005, Grier 2005]. The genes

expressed during embryonic development are believed to regulate cellular proliferation, migration and differentiation; however in the adult, it seems they play a role in the maintenance of the differentiated state of the tissue.

Hox gene mis-expression has recently been linked to cell growth and carcinogenesis. In tissues expressing up-regulated *Hox* genes, the cells tend to be undifferentiated and growing at a more rapid rate. [Abate-Shen 2002] In cancerous tissues, some *Hox* genes normally possess tumor suppressive characteristics; instead the genes are silenced and thus down-regulated. Additionally, some tissues express *Hox* genes in aberrant patterns that similarly result in oncogenic effects. This deregulation of *Hox* genes causes many different types of cellular changes in which cells escape the normal growth pathways. Examples of cells escaping the normal pathways include: leukemias in which fusion-protein mediated over-expression of *Hox* genes promotes clonal expansion; neuroblastomas in which expression of a single *Hox* gene promotes differentiation and prevents tumorigenesis; and abnormal *Hox* expression drives overexpression through apoptotic escape, altering cell receptor signaling, epithelial mesenchymal transition, or tumor cell invasion. [Shah 2010]

For example, *Hox* B13 normally functions as a tumor suppressor gene that is necessary for the development of organisms. However, when B13 is expressed in an aberrant pattern, aggressive disease and tumorigenesis is observed. [Shah 2010] In addition to B13, there are several other genes that have some well-studied roles in oncogenesis. Loss of expression through promoter methylation of *Hox* A5 is found in more than 60% of breast cancers that arise with the loss of p53 functionality, cell cycle regulating “check-point”. In contrast, A1 is found to be up-regulated in neoplastic breast tissues. Similarly, B7 is overexpressed in breast and ovarian

cancers, as well as melanomas. A7 is highly activated in differentiated ovarian tissues of the epithelium. [Abate-Shen 2002, Samuel 2005, Shah 2010]

1.3.2: Post-embryonic and Oncogenic Roles: *Hox* Paralogs 8 and 9

In addition to the regulatory abilities of these genes in various pathways, the genes of paralogs 8 and 9 are also highly active in oncogenesis. For example, *Hox* genes closer to the 5' end of the chromosome, more specifically those of clusters A and D, have been linked to overexpression in primary carcinomas of the lung. [Shah 2010]

Hox A9, in both human and murine studies, has been linked to hematopoietic stem cell renewal and is thought to be a major component in myeloid leukemias, acute lymphoblastic and acute myeloid leukemias. *Hox* A9 has also been linked to hematopoietic stem cell expansion. [Thornsteindottir 2002] A9 overexpression is also correlated to a decrease in early B-cell development. Histone methylation and other modifications, initiated through a complex of DNA binding cofactors, deregulate A9. [Shah 2010, Thornsteindottir 2002] Similarly, B9 is associated with hematopoietic progenitor cells. This particular gene is linked to the inhibition of prosurvival factors, resulting in progenitor apoptosis. By inhibiting these pathways, progenitor cells were no longer able to survive, proliferate or differentiate. [Krishnaraju 1997]

However, paralog 8 and 9 genes of clusters A and D are not the only genes of these paralogs associated with carcinogenesis. *Hox* C8, when overexpressed in prostate cancers, results in the loss of function of tumor differentiation. This occurs through the suppression of androgen-mediated transcription. Androgen receptors are responsible for internalizing ligand hormones that function to bind DNA with these androgen-mediated transcription factors.

[Samuel 2005] It has also been shown that *Hox* B6, B8, C8 and C9 are overexpressed during various stages of colorectal cancer. [Vider 1997] The up-regulation of these genes was tested in 11 different types of tumors, varying in progression from pre-malignant polyps to Dukes' C metastatic tumors (see **1.4.2**). The results were compared to two non-colorectal tumors and to adjacent, non-tumorous, epithelial mucosa tissues. Additionally, the results were confirmed with HT29 and Caco-2 cells. The up-regulation of these genes coincided with a decrease in Cdx1. Cdx1, or caudal type homeobox 1, is a member of the caudal-related transcription factor gene family. The encoded protein CDX1 regulates gene expression specific to the intestines and differentiation of enterocytes. [Vider 1997]

1.4.1: The Colon

The colonic epithelium consists of crypts and villi. The crypt contains approximately 250 cells, while each villus is composed of nearly 3,500 cells. There are different cell types represented in both of these structures. Stem cells, or undifferentiated cells, are confined to the crypts. As the cells progress out of the crypts, they undergo differentiation into one of the four types of cells present in the epithelium. These differentiated cell types are: goblet, Paneth, enteroendocrine and absorptive cells [Figure 2]. Each of the cell types possesses distinct functions within the colon. For example, goblet cells are responsible for secreting mucin. Mucin dissolves

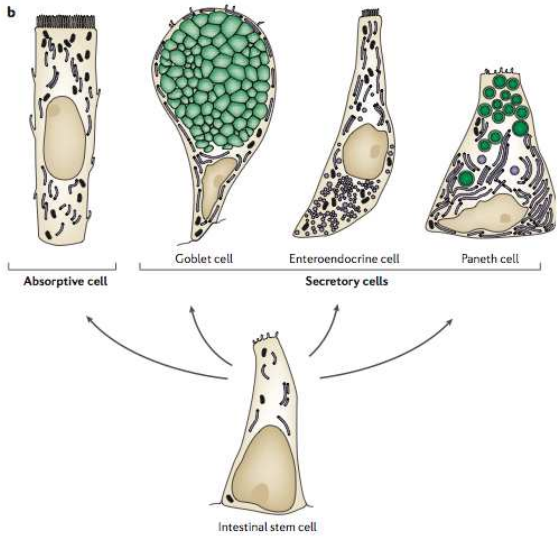

Figure 2. A schematic of the intestinal stem cell differentiating into the four possible cell types. From left to right: absorptive (columnar/enterocytes), goblet, enteroendocrine and Paneth cells. Reprinted by permission from Macmillan Publishers Ltd: Nature Reviews Genetics (Crosnier 2006), copyright 2006

in water and forms the epithelial mucosa of the colon. Paneth cells contribute to the maintenance of the gastrointestinal barrier by secreting anti-microbial substances into the lumen of the crypts, thus protecting the stem cells. Enteroendocrine cells are smaller and secrete hormones such as peptides and catecholamines. Absorptive cells, also known as enterocytes, are the only non-secretory cells found in the epithelia of the intestine or colon. These cells function in fluid transport, as well as ion, sugar, peptide, amino acid, lipid and vitamin B12 uptake. They also reabsorb excess bile. [Crosnier 2006]

In a "normally' functioning system, cellular renewal from the stem cells into one of the four types occurs. This is followed by the extrusion of the terminally differentiated cells into the lumen of the colon. During or after extrusion, the cells undergo apoptosis. This process usually occurs with 72 hours of the differentiated cell leaving the crypt. [Barnard 1993] However, in colorectal cancers the system goes awry and cells do not properly progress from the stem cells into differentiated cells. Instead, neoplastic tissues form and the cells maintain an undifferentiated, proliferative state in which none of the four differentiated cell types are represented.

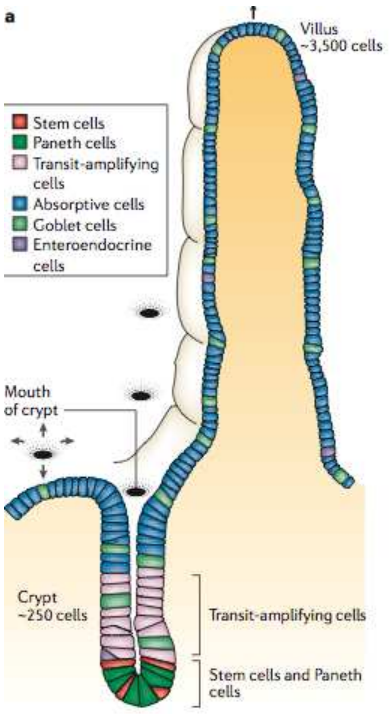

Figure 3. The diagram displays the location of the different types of cells within the epithelium of the colon, in the crypts and villi. Reprinted by permission from Macmillan Publishers Ltd: Nature Reviews Genetics (Crosnier 2006), copyright 2006

1.5.1: The Model: HT29

The HT29 (ATCC: HTB-38) cell line is derived from a grade II human colon adenocarcinoma. An adenocarcinoma is defined as a cancer of the epithelium of glandular

tissues. The classification of grade II refers to the stage of differentiation; II is an intermediate of moderately differentiated tumor. Due to the proliferative abilities of these cells in culture, they provide an excellent model for investigating the role of *Hox* genes in oncogenesis.

In a proliferative, undifferentiated state, HT29 cells grow in nonpolar multi-layers [Le Bivic 1987]. However, when modulated, these cells begin to acquire a differentiated phenotype similar to that of goblet and/or absorptive epithelial cells. These differentiated cells become polarized and grow as a monolayer. In this differentiated state, tight junctions with adjacent cells form basolateral and apical domains. [Cohen 1999] *In vitro,* differentiation is reversible dependent upon the environment. The modulation of cellular environment, also known as induced differentiation, is performed along a gradient in order to ensure the cells are not shocked by sudden changes and thus enter into apoptotic pathways. There are two common methods that are currently used in order to differentiate this cell line. The first is by introducing a sugar other than glucose, galactose. The second is by use of other chemicals, such as sodium butyrate or methotextrate.

Currently in this cell line, it is unknown which *Hox* genes are differentially expressed and whether there are direct role(s) of these genes on cellular fate. However, more conclusive research has been conducted in another colon adenocarcinoma cell line, Caco-2 [Freschi 2005]. Caco-2 (ATCC: HTB-37) exhibits similar morphological phenotypes upon differentiation. Differentiation in this cell line is referred to as spontaneous enterocytic differentiation, characterized by polarization, brush border formation and expression of hydrolases upon confluency *in vitro*. They also grow in monolayers with some dome-cluster formation, like HT29. It was observed that *Hox* genes of the A and C clusters are differentially expressed in the sister cell line, Caco-2 [Freschi 2005]. In normal adult colon tissue samples, *Hox* A genes are

expressed in proliferating cells of an undifferentiated nature in the base of the crypts of the epithelium. The expression of *Hox* C genes is localized to the apex of the crypts of the colonic epithelia. [Freschi 2005]

Additionally, research has been conducted in colorectal cancer sample tissues from patients with familial adenomatous polyposis (FAP), Dukes' A, B and C tumors. Whereas FAP is usually an inherited condition in which benign polyps form on the epithelia of the colon, Dukes' tumors are malignant tumors. As malignancy indicates the ability of these tumors to metastasize, the Dukes' system of tissue classification refers to the stage or progression of the cancer. For example, A and B indicate that the cancer is established in the lining of the colon or has grown through the muscular layer. C and D are indicative of metastases to the lymph nodes and/or other parts of the body, respectively. [Eschrich 2005, O'Connel 2004] Using these tissues, the researchers identified possible deregulated *Hox* genes by nucleotide sequencing of RT-PCR detection products, in comparison to those of adjacent non-tumorous colonic mucosa tissues [Vider 2007]. It was determined that *Hox* B6, B8, C8 and C9 are up-regulated at various stages in the development of these cancers [Grier 2005, Vider 1997]. Following identification of up-regulated genes, the group verified their data in cell culture lines HT29 and Caco-2. They also attributed the differentiated phenotypes of the cell lines to regulation of Cdx1 (see **1.2.3**). [Vider 1997] In addition to Cdx1, Cdx2 is linked to regulating intestine-specific gene expression and differentiation of enterocytes. [Guo 2004] CDX2 is expressed in the development of the gut during embryogenesis and throughout adulthood. CDX2 is a member of the homeobox family expressed in fully differentiated tissues. In colorectal carcinomas, CDX2 loses protein expression. [Samuel 2005] However, overexpression of this protein promotes intestinal cell differentiation and marked decrease in the ability to proliferate [Abate-Shen 2002]

1.5.2: The Model: Induction of Differentiation and its Implications

As previously mentioned, differentiation of cells can be induced by certain types of treatment. In the HT29 cell line, because the cells are derived from a moderately differentiated tissue, they possess some features of differentiated cells. The American Type Culture Collection from which this cell line was obtained states that one of the observed ultrastructural features includes microvilli and that mucin expression is present. Both of these characteristics are also associated with differentiated cells. However, they are not fully differentiated. They still possess the ability to become one of the four types of cells found present in the epithelium of the colon. [ATCC, Crosnier 2006, Huet 1967]

The mechanisms by which differentiation can be induced are not yet fully understood. Researchers Augeron and Laboisse stated that cancer cells of a somatic nature, or cells not related to reproductive tissues and organs, are useful models for studying induced differentiation roles and cellular characteristics. These cancer cells are classified into three general categories based on their abilities to differentiate due to 1) nutritional condition changes, 2) short-term treatment with chemicals, or 3) response to naturally occurring chemicals found within the body. [Augeron 1984] For this research, the mechanism of choice was treatment with a chemical known as sodium butyrate (NaBT). Sodium butyrate is a known histone deacetylase inhibitor. [McCue 1984] Acetylation and deacetylation of histones occurs on the lysine residues. When the histone is acetylated, usually by an enzyme known as acetyltransferase, the chromatin is loosely packed or in an "open" conformation. This allows for transcription and other processes to occur. If the histone is deacetylated, by the enzyme deacetylase, the histone is in a "closed" position and the chromatin is densely packed. These processes of acetylation and deacetylation are highly regulated. [Privalsky 1998, Ruijter 2003]

While not specific to HT29, in mouse embryonic carcinoma cells treated with NaBT showed a marked increase of acetylation on histones 3 and 4 (H3 and H4). [McCue 1984]

The goal of this research was to determine the effects of sodium butyrate, known histone deacetylase inhibitor on *Hox* gene expression in human adenocarcinoma colorectal cancer cell line, HT29. The hypothesis was that *Hox* genes expressed only in untreated HT29 cells are responsible for maintaining the proliferative, undifferentiated state of these cells. The first objective was to identify the pattern of expression of all 39 *Hox* genes in untreated and sodium butyrate treated HT29 cells by use of reverse transcription polymerase chain reaction (RT-PCR). Due to the role of sodium butyrate as a possible differentiating agent, the second objective was to target select genes with a distinctive pattern of expression that may play a role in maintaining the undifferentiated state of the tissue. For example, these genes would be expressed in untreated HT29, but not treated HT29. The expression of these targeted genes were quantitatively analyzed by use of quantitative real-time PCR (qRT-PCR), normalized against housekeeping genes. The protein expression of these targeted genes were also studied by use of Western blot. Additionally, another objective was to determine the effects of sodium butyrate on the cellular phenotype. If the sodium butyrate was effectively differentiating the treated HT29 cells, the cells should exhibit phenotypes similar to that of one of the four cell types found in the epithelium of the colon. These phenotypes include the formation of brush borders, apical and basolateral domains, and tight junctions. This was performed by ultrastructural analysis of untreated and NaBT treated HT29 cells in transmission electron microscopy (TEM).

Chapter 2: Materials and Methods

The following techniques were applied to this research and were carried out within laboratories of the Howell Science Complex at East Carolina University.

2.1.1: Cell Culture: Untreated HT29

The HT29 cells (ATCC: HTB-38) were cultivated in Dulbecco's Modified Eagle Medium (DMEM/F12) (Gibco 113300), supplemented with 10% fetal bovine serum (FBS), 100 U penicillin/100 μg streptomycin (Gibco 15140) and 1 mM sodium pyruvate (Gibco 11360).

The cells were maintained in medium and split upon 60-75% confluency. Splitting was done by washing the cells with 1X PBS (Phosphate Buffered Saline) upon aspirating and discarding the media. The cells were rinsed with 0.5% Trypsin/EDTA and incubated at room temperature until the cells detached from the flasks. The cells were resuspended in fresh DMEM/F12 and seeded into new flasks. The media was changed every other day.

2.1.2: Cell Culture: Sodium butyrate-treated HT29

For sodium butyrate-treated HT29 cells, a media containing sodium butyrate was used. The treated HT29 cells were cultivated in DMEM/F12, supplemented with 10% FBS, 100 U penicillin/100 μg streptomycin, 1 mM sodium pyruvate and 5 mM sodium butyrate (Sigma-Aldrich B5887). The introduction of sodium butyrate (NaBT) media in treating these cells was performed following the guidelines of Table 1.

Table 1. Treatment of HT29 cells with sodium butyrate containing media. Adapted. [Augeron et. al 1984]

Day of Treatment	Media Conditions
Days 0-1	Standard Media (DMEM/F12)
Days 2-7	5 mM Sodium butyrate supplemented DMEM/F12

Day 0 indicates the day on which the cells (untreated) were split and seeded into new flasks by the same previous methods. However, for sodium butyrate treatment, the densities of seeding are as follows:

T25: 1.5-2.0 x 10^6 cells per flask
T75: 6.0 x 10^6 cells per flask
35 mm petri dish: 7.7 x 10^5 cells per dish
Other sizes: 10,000 cells/cm^2

Control untreated HT29 cells were also seeded at the same densities. The NaBT media was changed on days 1, 2, 3, and 5 of each respective treatment.

2.1.3: Cell Culture: Cell Growth Curves

In order to determine the number of cells present in a flask on varying days of growth after seeding, cell growth curves were used. This procedure was also a good indicator of cellular proliferation and/or death during NaBT treatment. The untreated HT29 cells served as the control.

On Day 0, 9.6 x 10^4 HT29 cells were seeded into 35 mm petri dishes. For a seven-day growth curve, each day had three replicates of each untreated and treated HT29. Over the course of the seven days, the untreated HT29 were maintained with fresh media every other day (see **2.1.1**). The NaBT treated HT29 cells were maintained with the supplemented media as

previously stated (see **2.1.2**). On days 1, 2, 3, 5 and 7, the replicates of both untreated and treated cells were counted.

The media was removed from the petri dishes and discarded. The cells were rinsed with 1X PBS and 1 mL 0.05% trypsin/EDTA was pipetted into the petri dish. Allowing enough time incubating for the cells to detach, fresh media was added to the existing trypsin/cell suspension. The volume was dependent upon the number of cells in the petri; initially, 1 mL was sufficient, progressing to 2 mL toward the end of the seven-day period. The mixture was pipetted well in order to break apart clumps of cells. 50 μL of cell suspension was transferred from the petri dish to a 1.5 mL microcentrifuge tube. 5 μL Trypan Blue dye was added to the tube, in addition to 45 μL of 1X PBS. The sample was triturated by use of pipet and 20 μL was loaded into a haematocytometer. The cells were then counted and the procedure was repeated for all of the petri dishes harvested.

2.2.1: RT-PCR: RNA Extraction

Cells were lysed and total RNA was extracted with the Qiagen™ RNeasy™ kit following manufacturer's instructions with slight modifications.

First, the HT29 cells were seeded in a T75 flask at a density of 6×10^6 cells. The flasks were then sodium butyrate treated (see **2.1.2**). On day 4 of treatment, untreated HT29 cells were seeded at the same density of 6×10^6 cells and maintained (see **2.1.1**). On day 7, both the untreated and treated flasks were harvested for RNA extraction. The media was aspirated and discarded, and the cells were rinsed with 1X PBS. The flasks of cells were then lysed with RLT lysis buffer by scraping with a rubber policeman. The lysate was pipetted into tubes at a volume of ~500 μL, each. Each tube of lysate was homogenized through an RNase-free 21½ gauge

sterile needle, by aspiration 6-7 times. 1 volume of 70% ethanol was added to each tube of lysate, mixed and transferred to a spin column. The samples will be centrifuged for 15 seconds at 10,000 rpm and the flow-through will be discarded. This step was repeated until all of the sample was added. At this step, an optional RNA DNase treatment was performed. 350 μL buffer RWI was added to the column, followed by centrifugation for 15 seconds at 10,000 rpm; the flow-through will be discarded. 10 μL DNase I stock solution was mixed with 70 μL buffer RDD in a new PCR reaction tube; the mixture was then briefly centrifuged. The sample was loaded onto the column and incubated on the bench top for 15 minutes. Following this incubation, 350 μL buffer RWI was added to the column and centrifuged at 10,000 rpm for 15 seconds. The flow-through was discarded. Following DNase treatment, 500 μL of RPE buffer was added and centrifuged for 2 minutes at 10,000 rpm. The flow-through was again discarded and followed by centrifugation for 1 minute at 10,000 rpm in order to remove residual ethanol. The column was transferred to a fresh tube; RNA was eluted with 30 μL RNase-free water and again centrifuged for 2 minutes at 10,000 rpm. If the optional on-column DNase treatment was not performed, an off-column DNase treatment was performed after RNA elution. The eluted RNA was DNase treated with 0.1 of RNA volume 10X Turbo buffer and 1 μL Turbo DNase. The RNA was incubated at 37°C for 30 minutes. Then, 0.1 volume inactivation reagent was added, mixed constantly, and incubated at room temperature for 5 minutes. Following the incubation, the sample was centrifuged at 10,000 x g for 1.5 minutes. The supernatant was removed and put into a new tube and was used for quantification. The pellet was discarded.

After determining the concentration using the ThermoScientific NanoDrop™ 2000 Spectrophotometer and NanoDrop software, the RNA was stored at -80°C.

2.2.2: RT-PCR: cDNA Synthesis

In a PCR tube, 1 μg RNA, 1 μL 10 mM dNTPs, 1 μL random hexamer primers, and water to a total volume of 10 μL was mixed. The mixture was incubated at 65°C for 5 minutes. The samples were cooled briefly on ice, centrifuged, and a mixture of the following was added: 4 μL 5X First Strand Buffer, 2 μL 0.1 M DTT, and 1 μL RNaseOUT™. The sample was incubated at 25°C for 2 minutes, followed by the addition 1 μL SuperScript™ II RT.

The sample was incubated at 25°C for 10 minutes, followed by 42°C for 50 minutes and 70°C for 15 minutes. 1 μL of 2 U/μL *E. coli* RNase H is added and incubated for 20 minutes at 37°C.

The cDNA was cleaned using the Qiagen™ MinElute™ kit. Five volumes of buffer PB was added to the cDNA and loaded onto a to a MinElute™ column. The column was centrifuged at 13,000 rpm for 1 minute and the flow-through is discarded. Then, 750 μL buffer PE was added to the column and centrifuged at 13,000 rpm for 1 minute and the flow-through was discarded. A dry spin followed with centrifugation for 1 minute at 13,000 rpm. The column was transferred to a new tube, 10 μL RNase-free UltraPure water was added and incubated on the benchtop for 10 minutes at room temperature. The cDNA was eluted by centrifugation for 1 minute at 13,000 rpm. The final volume was adjusted to 20 μL with RNase-free UltraPure water. The NanoDrop software was used to determine the concentration of the cDNA. The cDNA was stored at -20°C.

2.2.3: RT-PCR: Genomic DNA Extraction

In order to test primers or cDNA samples for genomic contamination, genomic DNA extractions were performed. The cells were lysed with SB lysis buffer (containing 50 mM

HEPES (pH 7.5), 150 mM NaCl, 1 mM $MgCl_2$, 1.5 mM EDTA, 0.5% Triton X-100, 20 mM β-glycerolphosphate, 100 mM NaF, 0.1 mM PMSF) and scraped with a rubber policeman. The contents were then transferred to a 1.5 mL tube. 2 μL 10 μg/mL proteinase K was added to the sample, mixed and incubated in a 50°C water bath for 2 hours.

1 volume PCI (25:24:1 phenol chloroform isoamyl alcohol) was added to the tube and centrifuged at 12,000 rpm for 5 minutes. The aqueous layer was carefully removed and transferred to a new tube, repeating the procedure above. To the isolated aqueous solution, 4 volumes of 0.3 M potassium acetate were added, followed by two volumes ethanol and stored at -20°C overnight. The tube was centrifuged for 5 minutes at 12,000 rpm. The DNA pellet was then washed with 70% ethanol and centrifuged. The DNA was dried, resuspended in 50 μL 0.5% Tris/EDTA and incubated overnight at 37°C. The concentration will be quantified using NanoDrop software as before and the gDNA was stored at -20°C.

2.2.4: RT-PCR: Preparation and Analysis

Reverse transcriptase polymerase chain reaction (RT-PCR) was used to determine the pattern of expression of *Hox* genes in both untreated and treated HT29 cells.

A mixture of the following was prepared: 1 μL cDNA, 2.5 μL 10X PCR, 0.75 μL 50 mM $MgCl_2$, 0.5 μL 10 mM dNTPs, 2.5 μL respective 3 pmol/μL primer F, 2.5 μL respective 3 pmol/μL primer R, and the volume was adjusted to 20 μL with RNase-free UltraPure water; finally, 0.65 U Taq polymerase was added.

ß-actin was used as the positive and negative controls; the negative control contained no cDNA template, instead replacing that volume with additional water. The mixtures were then processed in the Thermalcycler for the following cycles:

Step 1: 94°C 00:04:00
Step 2: 94°C 00:01:00
Step 3: **°C 00:00:45
Step 4: 74°C 00:01:00
Step 5: go to step 2, x 39
Step 6: 74°C 00:10:00
Step 7: 15°C hold step

The annealing temperature** for each mixture was specific to the set of primers used. (Table 2)

Following RT-PCR amplification, the products were analyzed with gel electrophoresis. Using 0.75 grams of agarose, a 1.5% gel was prepared with 50 mL 1X TAE buffer (Tris base/acetic acid/ethylenediamminetetraacetic acid: 3.3 M TrisBase, 50 mL 0.5 M EDTA, 55 mL glacial acetic acid, brought to a final volume of 500 mL with ddH_2O).

Once the gel electrophoresed, it was drained of buffer and photographed with a Kodak 1D-imaging device using Carestream Imaging software.

Table 2. Primers, cDNA sizes, corresponding annealing temperatures. Primers highlighted in gray indicate intron-flanking sequences. *Primers A3, A4 and D11 were purchased from Santa Cruz Biotechnology, Inc. and the sequences are considered proprietary.

***Hox* Gene**	**Size (bp)**	**Temperature (°C)**	**Primer Pair Sequences**
A1	360	60.5	+GGCGTGGAGAGGGGACAAGGAG -CACCACCACCACCACCACCATC
A2	102	54	+ACAGCGAAGGGAAATGTAAAAAGC -GGGCCCCAGAGACGTAA
A3	470	60	**
A4	559	54	**
A5	293	55	+CCCCTCTCTGCTGCTGATG -CCATTGTAGCCGTAGCCGT
A6	511	63.1	+CCGGGAGCCTTCCCAGCGGC -GCGGCGCCGTGTCAGGTACGC
A7	225	55	+GGGGATGTTTTGGTCGTA

			-GCGGGGGCTTCTCTGTTC
A9	549	55	+ATGGAGGAGGTATTGTAATGC -CCCGCATTTTTAAGGTGGAG
A10	542	55	+GTGAAAACGCAGCCAACTGG -CAGGACTTGACACTTAGGAC
A11	415	55	+AGCAAATCCACTCCTCTAAG -GCTTTTTTACTCAGGGGTCC
A13	233	55	+CTGGAACGGCCAAATGTACT -AGAGATTCGTCGTGGCTGAT
B1	260	56	+CCTCGGGGTATGCTCCTG -GGGTGTTTCCTTGTCCTC
B2	145	50	+CCTTCCCCGCTGTCTTGG -GCTCGCTTTTGGCTCCTG
B3	227	50	+CCCCCAACCCCCATTTCA -CGCCCCCATTACTGCTGT
B4	161	60	+GTGCAAAGAGCCCGTCGTCTACC -CGTGTCAGGTAGCGGTTGTAGTG
B5	659	58	+GCTCTTACGGCTACAATTACAATG -GCTCAGCCAGGCTCATACT
B6	225	56	+AAGAGCAGAAGTGCTCCACT -TGATCTGCCTCTCCGTCA
B7	459	60	+CGGGCGCTTCCTTCGCCGCC -CCCGGGCCCGCGGTCTTGTTC
B8	291	55	+TTCTACGGCTACGACCCGCT -CGTGCGATACCTCGATTCGC
B9	600	55	+CCTTTGCCCTTACCTGTCTC -GCTCCACCTAAGATAGCTTC
B13	544	60	+TGACCAGCCACCCAGCGGCG -TGCGGCCGCGACGAAAGGCG
C4	510	64.2	+CACCGCCTCCGCGCCCTAGC -CGGCCGGGGGTGCTGACCTG
C5	481	56.6	+TCCTCCCCAACGTCGCCCTC -TGTCGCTCGGTCAGGCAAAGC
C6	317	58	+CACCTTAGGACATAACACACAGACC -CACTTCATCCGGCGGTTCTGGAACC
C8	267	55	+TCAGAGCGTGGGCAGGAG -GCGGAGGATTTACAGTCG
C9	114	60	+ACGAGGAAGAAGCGCTGCCCC -GAGAACCCGGGCCACCTCATA

C10	369	55	+CCTCCTGCTCCTACCCACCTA -GGCTCGGTCCGTCTTGATTT
C11	195	55	+CCTCCTTCCACCGTCACC -GTCGCCGCCACCGCAGTA
C12	124	60	+TAATCTCCTGAATCCCGGGTTT -TGGGTAGGACAGCGAAGGC
C13	417	60	+TGTCGCACAACGTGAACCTG -CTTCAGCTGCACCTTAGTGTAG
D1	210	57	+TTCAGCACGTTCGAGTGGAT -TGCGTGTCATTCAGGTGCAA
D3	187	54	+CATCAGCAAGCAGATCTTC -AGCGGTTGAAGTGGAATTC
D4	271	56	+TGGATGAAGAAGGTGCACGT -TAGAGTTTGGAAGCGACTGT
D8	219	56	+GGATACGATAACTTACAGAGAC -TAGAGTTTGGAAGCGACTGT
D9	285	56	+GAGTTCTCGTGCAACTCGT -CAGCTCAAGCGTCTGGTAT
D10	541	50	+CCTACAAAGGACACAATCTC -GTACTCTTGGGTTTTCCCGG
D11	549	64	**
D12	383	57	+AGCAGGCTAAGTTCTATGCG -CAATCTGCTGCTTCGTGTAG
D13	407	52	+CCCCCAGCCAAAGAGTGC -CCGTTAGCCAGCGTCCAG

2.3.1: qRT-PCR: Cells-to-C_T Preparation

qRT-PCR was used to quantitatively determine the levels of expression of *Hox* D8 and D9 when normalized to a battery of housekeeping genes in both untreated and sodium butyrate treated HT29 cells.

Untreated and treated HT29 cells were harvested and prepared for qRT-PCR following manufacturer's guidelines with slight modifications using the Applied Biosystems Power SYBR® Green Cells-to-C_T™ kit (Life Technologies 4402953M).

On Day 0, 6 x 10^6 cells were seeded into each of five T75 flasks to begin sodium butyrate treatment (see **2.1.2**). On day 4 of treatment, untreated cells were seeded into five T75 flasks at the same starting density of 6 x 10^6 cells per flask, in order to ensure the cells were in a proliferative state at the time of harvesting. On day 7 of treatment and maintenance, both sets of cells (untreated and treated) were collected and a cell count was performed for each flask. The cells were first washed with 1X PBS after aspirating and discarding the media. The PBS was then removed and 2 mL of 0.05% trypsin/EDTA was pipetted into each flask. The cells were rinsed with the solution and it was removed. Into each flask, 2 mL of 0.05% trypsin/EDTA was added and the cells were incubated for a few minutes until detached. One mL of fresh DMEM was added to the flask to inactivate the trypsin/EDTA and the contents were transferred into 10 respective 15 mL conical tubes. The tubes were centrifuged to pellet the cells. The supernatant solution was aspirated, leaving the pellet to be suspended in 1-5 mL dependent upon pellet size. During the preparation and count, the cells were kept on ice. After performing the cell count and calculating the number of cells in each suspension, the cells were then pelleted in the centrifuge again. The supernatant was removed and the cells were washed in 4°C 1X PBS at a volume of 0.5 mL per 10^6 cells. The cells were again gently pelleted and the supernatant PBS was removed. The cells were kept on ice and resuspened in 4°C 1X PBS so that 5 μL contained 10^5 cells. The 5 μL volume of PBS/cells was transferred to a 0.250 mL nuclease/RNase-free PCR reaction tube. Each respective tube was labeled according to treatment type: treated or untreated, and flask number.

A DNase I 1:100 lysis core solution was prepared for each tube.

49.5 μL lysis buffer
0.5 μL DNase I

When calculating the total core volume (the above volumes are per tube), a 10% overage was factored in. To each PCR reaction tube of cells in 1X PBS, 50 μL of the DNase I lysis solution was added and pipetted to mix 5 times, ensuring no bubble formation. The tubes were then incubated at room temperature for 5 minutes. To each of the tubes, 5 μL of stop solution was added and pipetted to mix 5 times, ensuring no bubble formation. The tubes were incubated at room temperature for 2 minutes. The lysates could be stored on ice up to 2 hours or at -20°C or -80°C for up to five months.

An RT Master Mix core was prepared for transcribing lysates to cDNA, allowing for a 10% overage, the volumes below are per tube.

25 μL 2X SYBR RT Buffer
2.5 μL 20 X RT Enzyme Mix
12.5 μL Nuclease-free H_2O

The mix was kept on ice until use. For each reaction, 10 μL of prepared lysate was added to 40 μL of the RT Master Mix in a 0.250 mL PCR reaction tube. The reactions were then mixed gently by pipetting and briefly centrifuged to collect at the bottom. The tubes were incubated at 37°C for 60 minutes for the reverse transcription step, followed by an incubation at 95°C for 5 minutes to inactivate. The cDNA could then be held at 4°C for immediate use or -20°C for storage.

2.3.2: qRT-PCR: Templates, Plate Loading, Performing the Trials

The template, called RT reaction (cDNA), was prepared for the trials of qRT-PCR by diluting into 1:4, 1:20 and 1:100 with UltraPure water (Gibco 10977-023).

For each gene, D8, D9 and the seven housekeeping genes, three trials were performed. Each trial was untreated and treated template in the three varying dilutions, with three replicates per dilution. For each gene, a Power SYBR core mix was prepared, with a 10% overage calculated. The volumes below are per well of a 96-well PCR plate.

10 μL Power SYBR Master Mix
1 μL forward primer
1 μL reverse primer
4 μL Nuclease-free H_2O

Because the Power SYBR Green Master Mix is light sensitive, the exposure to light was kept as minimal as possible. The core was prepared in a 0.250 mL nuclease/RNase-free PCR reaction tube. The core tubes were kept on ice until use. From each Power SYBR core, 16 μL was pipetted into each of the wells needed in a 96-well PCR plate. To each well containing the core mixture, 4 μL of the respective diluted template was added and mixed by pipetting. The diagram below depicts the way the plates were loaded for the gene being tested (Figure 4). All three trials for each gene of interest were tested on the same plate.

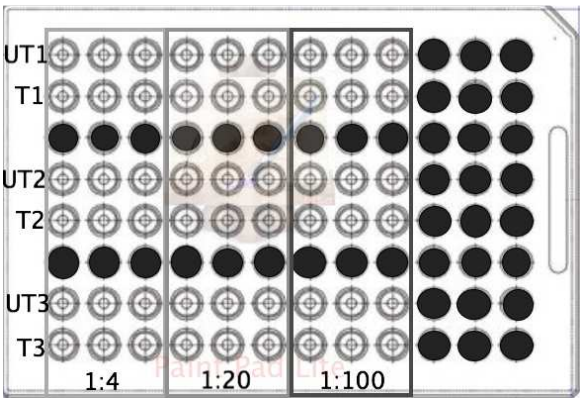

Figure 4. Diagram of the 96-well PCR plate. Darkened wells represent blank or unused wells. Each of the three trials on the plate contains 1 untreated (UT) row and 1 treated (T) row. There are three replicates for each dilution outlined.

The plate was then sealed using Biorad Microfilm 'B'. Using a Biorad C1000 Thermalcycler and corresponding software, Biorad CFX96 Real-time PCR Detection System, the plates will be run using the following settings:

Step 1: 95°C 00:10:00
Step 2: 95°C 00:00:15
Step 3: **°C 00:01:00 + plate read
Step 4: go to step 2, x 39
Step 5: melt curve 65-95°C at 0.5°C increments for 5 seconds + plate read

The asterisks(**) in step 3 denote that the temperature used was primer specific. (Table 3) In addition, negative controls that replaced the template volume with water were run for each gene of interest and housekeeping gene. Once used, the plates were stored at -20°C and the output data was used for analyses with Pfaffl.

Table 3. qRT-PCR primer sequences, annealing temperatures and amplicon sizes for two sets of designed *Hox* paralog 8 and 9 genes and housekeeping genes. The asterisks (**) denote the two primer pairs used for D8 and D9 gene of interest trials. The (-) denotes genes for which conditions were not tested or are unknown.

Gene	Identification	Primer Pair Sequence	T_m (°C)	Amplicon Size (bp)
A9	Forward1	CCGCGGATGAGCTGAGCGTT	55	103
	Reverse1	CTGCACGGGCTGAAGTCGGG		
	Forward2	GAGAGCGGCGGAGACAAGCC	55	75
	Reverse2	CCGAGTGGAGCGCGCATGAA		
B8	Forward1	TTCTGTGTGTGAGCTACCGTGGAT	60	84
	Reverse1	CGAGGGAGCCTTTGCTTAAATCCT		
	Forward2	CAGAACCGGAGGATGAAGTGGAAA	-	154
	Reverse2	AAGCCTACTTCTTGTCGCCCTTCT		
B9	Forward1	TGCAAATACCCACCAGGGAGATGT	60	90
	Reverse1	ATGGGAATGGTATGGCAATGCTGC		
	Forward2	CGCGTCCGAAAGCCCTCACAC	-	98
	Reverse2	ATTATCCGGGCGCTTGCAGGG		
C8	Forward1	AACTGTCTCCCAGCCTCAGTTT	60	86
	Reverse1	TGATACCGGCTGTAAGTTTGCCGT		
	Forward2	TGGAAACCTGAAGGAGATGTGGGT	-	138
	Reverse2	AAACAGCGAAGGAGAGGAAGGCAT		
C9	Forward1	TCTTGCGATTTGGGAGGGTTCAGT	-	122
	Reverse1	GTCATTTATTTCGGTTGCGCTGGG		
	Forward2	ACAATGAAGACCTCCTAGCGTCCA	-	94
	Reverse2	AAATCGCTACAGTCCGGCACCAAA		
D8	Forward1	ACTTGTAGTCCAGCTCTGCAGCTT	65	142
	Reverse1	TACAAGGCGATTTGCCAGAGTTGC		

	Forward2**	TCGCTAGTTCTTTATGCGGTGGCT	65	91
	Reverse2**	GCGGCGAACAGAACAAAGGCAATA		
D9	Forward1**	AGCAGCAACTTGACCCAAACAACC	65	107
	Reverse1**	TTTCTCCAGCTCAAGCGTCTGGTA		
	Forward2	GCGAACTAGTCGGTGGCTCGG	65	80
	Reverse2	CGTCCCGCACTCCCACCCAA		
TFRC	Forward	AGGTCGCTGGTCAGTTCGTGATTA	60	82
	Reverse	AGCAGTTGGCTGTTGTACCTCTCA		
ACTB	Forward	AATGTGGCCGAGGACTTTGATTGC	63	93
	Reverse	AGGATGGCAAGGGACTTCCTGTAA		
B2M	Forward	AGATGAGTATGCCTGCCTGTGAA	57	82
	Reverse	TGCTGCTTACATGTCTCGATCCCA		
GAPDH	Forward	GAAGGTGAAGGTCGGAGTCAAC	66	70
	Reverse	CAGAGTTAAAAGCAGCCCTGGT		
TBP	Forward	TGATGCCTTATGGCACTGGACTGA	60	86
	Reverse	CTGCTGCCTTTGTTGCTCTTCCAA		
RPL13a	Forward	CCTGGAGGAGAAGAGGAAAGAGA	57	125
	Reverse	TTGAGGACCTCTGTGTATTTGTCAA		
RPLP0	Forward	GCAATGTTGCCAGTGTCTG	60	-
		GCCTTGACCTTTTCAGCAA		

2.3.3: qRT-PCR: Pfaffl Analysis

The output data from qRT-PCR was not in a form that was ready to be interpreted. In order to analyze the results, the data was first manipulated. The method for calculation is known as the Pfaffl method. [Livak 2001, Pfaffl 2001]

For each gene, both genes of interest (targets) and housekeeping (reference), the Biorad CFX Manager software provided a C_T value, or value at which the level of fluorescence exceeded the background levels and was detected. The C_T value for each replicate of each dilution was averaged. For example:

$$C_{T(avg)} = \frac{(C_{T1}+C_{T2}+C_{T3})}{\text{Number of Replicates}}$$

C_T data for a 1:4 dilution may have read: 24.30, 24.29 and 24.28. These values were averaged together: (24.30+24.29+24.28)/3 = 24.29, and this averaged value was used for further calculation.

A ΔC_T value was calculated for each dilution of the genes of interest ($\Delta C_{T(goi)}$) and reference genes ($\Delta C_{T(hkpg}$). For example:

$\Delta C_{T(hkpg)}$ $C_{T(avg)}$ untreated housekeeping gene - $C_{T(avg)}$ treated housekeeping gene

=

$\Delta C_{T(goi)}$ $C_{T(avg)}$ untreated gene of interest - $C_{T(avg)}$ treated gene of interest

=

These values were then used to determine the Pfaffl equation top and bottom lines. It is important to note here that the efficiency, when 100%, was equal to "2". If the efficiency was not equal to 100%, for example 94%, the value used was equal to "1.94".

$$\text{Ratio} = \frac{(E_{\text{target}})^{\Delta C_T(\text{untreated-treated})}}{(E_{\text{reference}})^{\Delta C_T(\text{untreated-treated})}}$$

The ratio was then the normalized level of expression of the treated gene of interest in comparison to the untreated gene of interest. This ratio was calculated for each dilution of each gene of interest against all of the reference genes.

The relative or normalized ratio was compared for each gene of interest, D8 and D9, to a housekeeping gene that was similar in C_T if available, and different in C_T. (Appendix A)

2.4.1: Transmission Electron Microscopy: Preparation of Solutions

Transmission electron microscopy was used to analyze the ultrastructural features of the untreated and sodium butyrate treated cells.

To prepare the Electron Microscopy Sciences® Embed™ Resin, 20 grams ERL-4221 (EMS®), 16 grams DER736 Epoxy Resin (EMS®), 50 grams NSA (EMS®), and 0.6 g DMAE (EMS®) were added together and stirred with a stir bar for 10 minutes. This solution was prepared right before use to prevent any hardening and was covered with Parafilm in order to prevent contamination.

To prepare the 0.1 M sodium cacodylate buffer, 250 mL distilled water was added to 250 mL 0.2 M sodium cacodylate buffer donated by the laboratory of Randall R. Renegar, PhD at the Brody School of Medicine department of Anatomy and Cell Biology. This solution was stored at 4°C until use.

To prepare the osmium tetroxide, one OsO_4 ampoule (EMS®) was added to 5 mL of distilled water and heated to dissolve. To this sample, 5 mL of prepared 0.1 M sodium cacodylate buffer was added and inverted to mix. This solution was stored at 4°C until use.

To prepare the 2% glutaraldehyde, one 10 mL ampoule of 50% glutaraldehyde (EMS®) was added to 240 mL of prepared 0.1 M sodium cacodylate buffer. This solution was stored at 4°C until use.

2.4.2: Transmission Electron Microscopy: Preparation of Cells

The cells were grown on 0.4 μm porous polyethylene terepthalate membrane (BD Falcon 35-3090) inserts placed in 6-well tissue culture treated plates. Sodium butyrate treated HT29

cells were seeded on the membranes and treated as previously stated in sodium butyrate supplemented DMEM/F12 (see **2.1.2**). On day 5 of sodium butyrate treatment, the untreated HT29 cells were seeded (see **2.1.1**). The cells were stored in a 37°C incubator + 5% CO_2. On day 7, both the untreated and treated cells were rinsed with 1X PBS and prepared for transmission electron microscopy (TEM).

The first fixation was performed with cold 2.0% glutaraldehyde in 0.1 M sodium cacodylate buffer for 30 minutes at room temperature. This initial fix was done leaving the membranes in the 6-well plate, working under the hood. The first buffer wash was with cold 0.1 M sodium cacodylate buffer, incubated at room temperature for 10 minutes. The buffer was removed and the wash was repeated two more times. The membranes were then postfixed using 1% osmium tetroxide (OsO_4) in 0.1 M sodium cacodylate buffer for 30 minutes, and was kept under the hood for the entirety of the incubation. The osmium tetroxide was then removed and the membrane was washed with 0.1 M sodium cacodylate buffer for ten minutes. The wash was repeated two additional times at room temperature. The membrane inserts were then transferred to new chambers of the 6-well plate to ensure no remaining water was introduced during dehydration. The first dehydration was with 30% ethanol for 10 minutes. During the dehydration steps, it was essential to leave the lid on the 6-well plate to reduce the introduction of environmental water into the system. Dehydration continued with the following ethanol variations, each for 10 minutes: 70%, 95% and 100%. Finally, dehydration was completed two washes in 100% ethanol for 20 minutes each. After the last dehydration step, the resin embedding procedures were performed on a shaker table to ensure the mixture was covering all parts of the membrane constantly. The epoxy used was Electron Microscopy Sciences®

Embed™ Resin. The membranes were embedded in increasing ratios of resin to 100% ethanol, as follows:

1 part Embed™ Resin to 2 parts ethanol x 30 minutes
2 parts Embed™ Resin to 1 part ethanol x 1 hour
3 parts Embed™ Resin with no ethanol x 1 hour, repeating three times total

After washing the membranes in resin, the final wash was removed from the membranes and the membranes were sectioned using fine-tipped scalpels.

The trimmed samples of membrane were placed into one of three different molds for embedding: BEEM capsule lids; flat, thin molds; or pyramidal shaped molds. The membranes were pushed firmly toward the bottom of each of the specific molds using an insect pin, carefully, as to not disturb the cells on the surface. The samples were pushed down so that the membrane was at the top of the block face and cells below so that blocks could be faced with the ultramicrotome without cutting away the cells. Membrane segments were embedded in the Electron Microscopy Sciences® Embed™ Resin.

An RMC MT6000-XL Ultramicrotome was used to obtain both thick and thin sections. The sections were cut with glass knives made with a Reicherto-Jung KnifeMaker II. Thick sections were mounted to glass microscope slides using EMS Permount. The sections were then imaged using a Leica CME phase contrast microscope. Thin sections were first expanded with toluene and then collected using a fine wire transfer loop to flame-sterilized 400 hexagonal mesh grids. For these particular preparations, thick sections were collected at a 990 nanometer thickness, while thin sections varied from 75-290 nanometers. Once dried, the grids were transferred to a multi-grid staining holder. The grids were stained with filtered uranyl acetate for 10 minutes at room temperature. Following staining, the grids were washed 3 times in distilled water, drying with a paper towel and Kimwipe between each rinse. The grids were then stained

with lead citrate in the dark in the presence of sodium hydroxide for 10 minutes. Following this second stain, the grids were washed 4 times with distilled water, again drying the grids between each rinse. One final wash in distilled water was performed and the grids were then dried. The grids were transferred to a piece of filter paper in a petri dish and left to dry completely.

The grids were stored until use, and then loaded into the Philips CM12 Transmission Electron Microscope for viewing and imaging. Micrographs for untreated HT29 cells were film negatives, which were then developed for analysis. Micrographs for treated HT29 cells were taken with AMT Custom Engineered Optics XR50 Digital Camera and analyzed using the imaging software AMT Image Capture Engine V602.

2.5.1: Western Blot: Preparation of Solutions

In order to determine if *Hox* D8 and D9 proteins are present in both untreated and treated HT29, and to further investigate their pattern of expression, Western blotting was performed. To perform these experiments, a number of solutions were first prepared. (Table 4)

Table 4. Necessary solutions prepared for Western blotting: RIPA lysis buffer for preparing cell lysates; 2X Laemmli buffer for a loading dye; transfer buffer for transferring the proteins from the SDS-PAGE gel to the PVDF membrane; TBST pH 7.6 for the preparation of antibody dilutions; electrode buffer for running the SDS-PAGE gel; 5% milk in TBST for preparation of antibody dilutions and blocking solution.

RIPA Lysis Buffer	2X Laemmli Buffer	Transfer Buffer
10 mM Tris-Cl pH 7.5	0.125 M Tris-Cl pH 6.8	48 mM Tris-Cl
150 mM NaCl	10% 2-mercaptoethanol	39 mM glycine
1 mM EDTA pH 8	20% glycerol	0.0375% SDS
1% NP-40	0.0004% bromophenol blue	20% methanol
0.1% SDS	4% SDS	
TBST pH 7.6	**Electrode Buffer**	**5% milk in TBST**
20 mM Tris-Cl	25mM Tris-HCl	1 gram fat-free powdered milk
140 mM NaCl	192mM glycine	20 mL TBST pH 7.6
0.1% Triton X-100	0.1% SDS	

2.5.2: Western Blot: Preparation of Whole-Cell Lysates

Day 0, 7.5 x 10^5 HT29 cells were seeded into three T75 flasks. These NaBT treated HT29 cells were maintained with the supplemented media as previously stated (see **2.1.2**). On Day 4, three T75 flasks of untreated HT29 were seeded at the same cell density of 7.5 x 10^5 and maintained with fresh media every other day (see **2.1.1**). Day 7, the untreated and NaBT treated cells were harvested for whole cell lysates.

The media was removed from the flasks and discarded; the cells were rinsed with 4°C 1X PBS. The PBS was aspirated and discarded, and 1 mL RIPA lysis buffer was pipetted into each flask. The contents were removed after scraping with a rubber policeman and placed into cold 1.5 mL RNase-free microcentrifuge tubes. 2 μL of protease inhibitor cocktail was added to each sample. The samples were then vortexed continuously for 20 minutes at 4°C. The tubes were then centrifuged at 4°C for 5 minutes at maximum speed. The supernatant was removed at stored at -80°C or used immediately for quantification by a Pierce 660 Assay.

The Pierce 660 Assay was performed using a 2 mg/mL standard of BSA. The sample tubes were prepared as follows. (Table 5)

Table 5. Pierce 660 Assay sample preparations. For the BSA standard, seven tubes are prepared using the appropriate volumes. The volume of protein used for these tubes is from the 2 mg/mL BSA stock. For the lysates, two tubes were prepared for each of the untreated and treated whole-cell lysates; the volume of protein used for these tubes is derived from the whole-cell lysate stocks.

	Tube	Vol. Pierce Reagent (mL)	Vol. H_2O (µL)	Vol. RIPA Buffer (µL)	Vol. Protein (µL)
BSA Standard	1	1	80	20	0
	2	1	70	20	10
	3	1	60	20	20
	4	1	50	20	30
	5	1	40	20	40
	6	1	30	20	50
	7	1	20	20	60
Lysates	1	1	80	10	10
	2	1	80	0	20

Once prepared, the samples were inverted to mix and incubated at room temperature for 5 minutes. The samples were then transferred to a 1 mL plastic cuvette before measuring and recording the absorbance (λ=660 nm). The machine used was a Shimadzu 1201 UV-Vis spectrophotometer.

2.5.3: Western Blot: SDS- PAGE

Resolving and stacking gels were first poured. For the D8 and D9 proteins, a 10% resolving gel and a 4% stacking gel were adequate. For the 10% resolving gel:

1.25 mL 40% acrylamide/bis-acrylamide (Biorad)
2.45 mL distilled H_20
1.25 mL 1.5 M Tris-Cl pH 8.8
50 µL 10% SDS
2.5 µL TEMED
25 µL 10% APS

After mixing the reagents in a 15 mL conical tube, approximately 5 mL (or to ~1 cm from the bottom of the comb when inserted) was pipetted into an assembled Biorad Gel Casting Tray

cartridge. Carefully, 70% ethanol was dispensed atop the resolving gel in order to prevent interaction with environmental oxygen. The gel polymerized at room temperature for one hour. The ethanol was removed and the 4% stacking gel was prepared:

0.25 mL 40% acrylamide/bis-acrylamide
1.6 mL distilled H_20
0.625 mL 0.5 M Tris-Cl pH 6.8
25 µL 10% SDS
2.5 µL TEMED
12.5 µL 10% APS

The reagents were mixed in a 15 mL conical tube and added on top of the resolving gel. The comb was inserted and the gel polymerized at room temperature for approximately 45 minutes. The comb was removed and the gel cartridge was transferred to a Biorad Mini-PROTEAN® Tetra Cell Tank assembly. The chamber was then filled with 1X electrode buffer; the wells were also rinsed with the electrode buffer.

Next, 10 µg of each respective untreated or treated cell lysate was added to an equal volume of 2X Laemlli loading buffer into 250 µL PCR reaction tubes. The solution was boiled at 95 °C for 5 minutes and briefly centrifuged. The gel was then loaded with 10 µL PageRuler™ Precision Plus pre-stained ladder (Thermoscientific) in the first lane, and the supernatant solution from the prepared samples of lysate/Laemelli loading buffer. Any empty or unused lanes were loaded with 10 µL of 2X Laemlli loading buffer. The SDS-PAGE gel was electrophoresed at 90 V for 1.5 hours, or until the dye and lowest band of the ladder had traveled to the near end of the gel.

2.5.4: Western Blot: Semi-Dry Transfer

After running the SDS-PAGE, the gel was removed from the cartridge, cutting the stacking gel from the resolving gel. The resolving gel was the only portion kept and used for the

remainder of the Western blot. The resolving gel was then rinsed in cold transfer buffer for 10 minutes. Additionally, 6 pieces of Whatman paper were soaked in transfer buffer for 5 minutes at room temperature after being cut to the appropriate size (a little larger than the size of the gel). Immobilon-P polyvinylidene difluoride (PVDF) membrane (Millipore) was cut to the size of the gel and soaked in cold 100% methanol for 1 minute. The PVDF membrane was then transferred to distilled water, soaking for 2 minutes, and finally to cold transfer buffer for 5 minutes. The transfer was then set up on the LKB© 2117 Multiphor II Electrophoresis Unit electrode plate. First, 3 of the 6 soaked Whatman paper sheets were laid down and rolled over with a glass stir rod to remove bubbles; a few milliliters of transfer buffer was poured over the top of the paper. The PVDF membrane was placed on top of the Whatman paper, followed by the SDS-PAGE resolving gel, ensuring that the gel only overlapped the membrane. The gel was topped with the three remaining pieces of Whatman paper, a few milliliters of transfer buffer, and subsequently rolled again using the glass stir rod. The extra transfer buffer was removed from the electrode plate using a sheet of heavy-duty filter paper. The top of the transfer apparatus was installed and the electrodes connected to a power source. The gel was transferred for 40 minutes at 200 mAmps. Following the transfer, the apparatus was opened, and the gel and filter paper were discarded. The membrane was kept for the remainder of the Western blot.

2.5.5: Western Blot: Blocking and Antibodies

From the transfer, the membrane was blocked with 5% milk in TBST buffer for 1 hour at room temperature on a shaker table. The membrane was then washed 5 times for 5 minutes, each at room temperature. After washing, the membrane was incubated in the primary antibody: mouse monoclonal IgG purified D8 or D9 (Novus Biologicals 10F8, 2A9) prepared at a 1:500

dilution with the 5% milk in TBST buffer for 4 hours at room temperature or up to overnight at 4°C. The primary antibody incubations were performed using a shaker table to ensure the solution covered the entirety of the membrane. The primary antibody solution was then discarded and a secondary antibody solution was added: a 1:5000 mouse horseradish peroxidase-conjugated antibody with the 5% milk in TBST for 1 hour at room temperature on a shaker table. The membrane was then ready for chemiluminescence (see **2.5.6**).

After chemiluminescence and imaging, the membrane was prepared for incubation with the loading control antibody. The membrane was stripped for 5 minutes at room temperature using a mild stripping buffer. Following the stripping wash, two washes for 10 minutes each in cold 1X PBS and two 5-minute washes in cold 1X TBST were performed. The PVDF membrane was then blocked following the same steps and incubated with a β-Actin primary antibody at a 1:5000 dilution with the 5% milk in TBST solution. The membrane was washed following the same steps and incubated with the mouse secondary antibody at a 1:5000 with the 5% milk in TBST solution. The membrane was again ready for chemiluminescence.

2.5.6: Western Blot: Chemiluminescence and Imaging

In order to visualize the presence of the targeted proteins, the Immobilon Western Chemiluminescent HRP Substrate Kit was used. The membranes were incubated in equal volumes of HRP substrate luminol reagent and HRP substrate peroxidase solution for 5 minutes at room temperature, with constant motion. The membranes were imaged using the BioRad ChemiDoc XRS+ System.

Chapter 3: Results and Discussion

3.1: *Hox* Gene Pattern of Expression and the Effects of Sodium Butyrate on Cell Growth

The first objective in this research was to determine the overall pattern of expression of *Hox* genes in the cell line HT29. This was done by performing RT-PCR on cDNA prepared from both untreated and sodium butyrate treated HT29 cells. cDNA from three different sets of both untreated and treated HT29 cells was used to perform replicates for each of the 39 genes tested. Once RT-PCR was performed, the samples were electrophoresed on a 1.5% agarose gel and the presence or absence of a band at the proper amplicon size was used to determine if the gene was expressed. For each set of cDNA tested, positive and negative controls using β-actin primers were used. The negative control did not contain any cDNA template.

The presence, '+', or absence, '-', of an amplicon band at the appropriate size for each *Hox* gene is compiled in the chart below. (Table 6)

Table 6. *Hox* gene pattern of expression in both untreated and NaBT treated HT29 cells. (+) indicates expression, (-) indicates no expression.

Gene	Untreated HT29 Expression	Treated HT29 Expression	Gene	Untreated HT29 Expression	Treated HT29 Expression
A1	+	-			
A2	+	+	**B13**	-	+
A3	+	+	**C4**	-	-
A4	+	+	**C5**	+	+
A5	+	+	**C6**	+	+
A6	+	+	**C8**	+	+
A7	+	+	**C9**	+	+
A9	+	+	**C10**	+	+
A10	+	+	**C11**	+	+
A11	+	+	**C12**	+	+
A13	+	+	**C13**	+	+
B1	-	-	**D1**	+	+
B2	+	-	**D3**	+	-
B3	+	+	**D4**	+	-
B4	+	+	**D8**	+	-
B5	-	+	**D9**	+	-
B6	+	+	**D10**	+	-
B7	+	+	**D11**	+	-
B8	+	+	**D12**	-	-
B9	+	+	**D13**	+	+

After analyzing the qualitative pattern of expression, the goal was to select a couple of genes of interest. The genes selected must show a differential pattern of expression in the untreated or treated HT29 cells. Many of the genes of cluster D were expressed in untreated HT29, but not in sodium butyrate treated HT29.

In addition to analysis of the RT-PCR results, a cell growth curve was performed in order to determine the effects of sodium butyrate on cellular growth and proliferation. If sodium butyrate is effectively differentiating the HT29 cells, it would be expected that untreated cells continue to exponentially proliferate and the treated cells would not. The cells were seeded at a

density of 9.6 x 10^4 cells/35 mm petri dish, as per the 10,000 cells/cm^2 guidelines adapted from Augeron *et. al*, 1984. The growth curve indicated that untreated HT29 cells began to proliferate on day 5, toward the end of growth curve period. However, growth in NaBT treated HT29 cells seemed to plateau in growth between days 2 and 3 of the seven-day treatment, and no longer proliferate (Figure 5).

The decrease in cell number between days 2 and 3 for both untreated and treated HT29 cells could be attributed to human error (pipetting of suspended cells on day 0, when all of the petri dishes were seeded). Also, the suggested cell density at which the untreated and treated cells were seeded is lower than optimal for normal growth.

The conclusions from the results of this graph show that untreated HT29 continue to proliferate, while sodium butyrate treated HT29 plateau and do not proliferate throughout the course of the treatment. This suggests that sodium butyrate prevents the proliferation of HT29 cells.

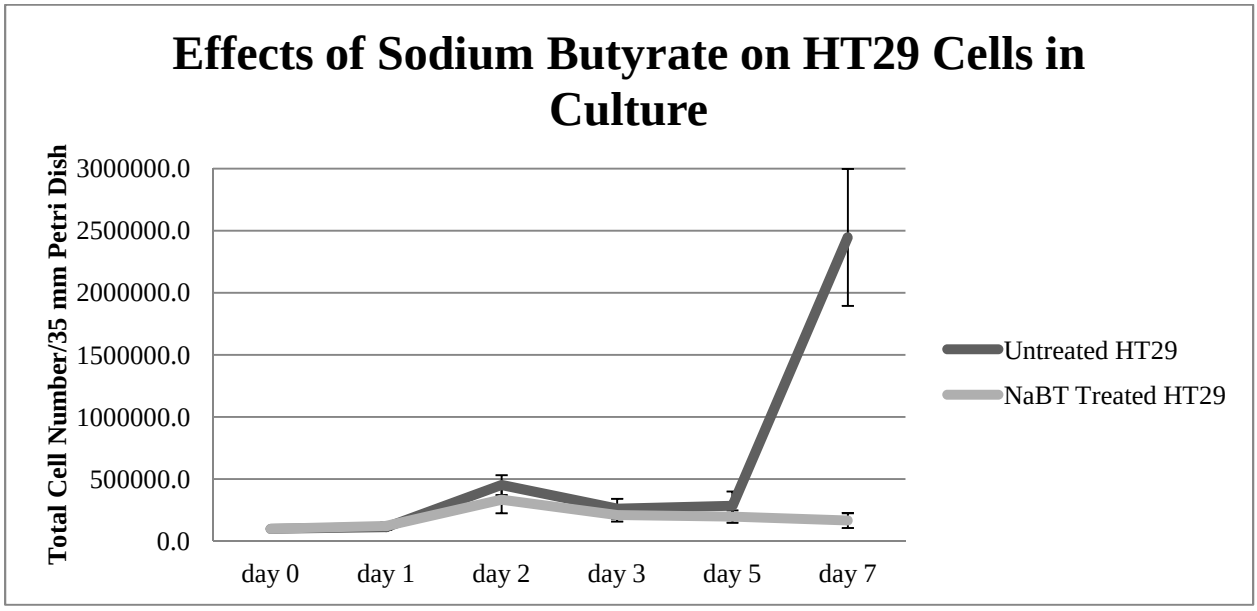

Figure 5. HT29 cell growth curve showing the effects of 5 mM sodium butyrate treatment over the seven-day treatment period. The cells were seeded into 35 mm petri dishes at a density of 9.6 x10^4 cells on day 0. Three petri dishes of each untreated and treated HT29 cells were harvested and counted for each day of the growth curve.

As stated in the literature, specific genes from paralog groups 8 and 9 are expressed during various stages of colorectal cancer. [Vider 1997] Additionally, *Hox* gene expression in cells that maintain the undifferentiated state are located at the base of the colonic epithelial crypts, where proliferation of stem cells occurs. [Freschi 2005] The preliminary results indicated that *Hox* genes D8 and D9 are expressed only in untreated HT29 cells and not in sodium butyrate treated HT29 cells, by RT-PCR. In correlation with the cell growth curve, the untreated HT29 cells continue to proliferate whereas treated HT29 cells do not. Thus, it was hypothesized that *Hox* genes D8 and D9 may be responsible for maintaining the proliferative state of untreated HT29 cells. Therefore, D8 and D9 were targeted for further investigation.

3.2.: *Hox* D8 and D9 Expression

The second objective was to determine the level of expression of D8 and D9 by use of quantitative Real-time PCR. These genes of interest were normalized to seven housekeeping genes and compared to determine the effectiveness of the Pfaffl method of calculation for the reactions. If the non-quantitative RT-PCR detection was an accurate representation of gene expression, the level of expression of D8 and D9 would be up-regulated in untreated HT29 cells and down-regulated or not expressed in NaBT treated HT29 cells.

The Pfaffl calculations (Appendix B) yielded a ratio of expression for sodium butyrate treated to untreated cells. Therefore, for each gene plot, the columns indicate the normalized level of expression of each gene of interest to the reference gene. In each dilution, an additional column “untreated D8” or “untreated D9” represents the normalized value of 1 for the untreated samples. (Figures 6-7) For comparison, two housekeeping genes were selected for each gene of

interest; one housekeeping gene with a C_T value close to that of the GOI, and the other with a C_T value differing from that of the GOI. The genes of interest were then normalized to these selected reference genes and analyzed. In Figure 6, *Hox D8* is normalized to β-Actin and TATA binding protein. ACTB has a higher level of expression in the starting quantity of 0.25 than in the other two dilutions: 2.4 as compared to 0.7. Additionally, TBP also has a higher level of expression at the template starting quantity of 0.25 than in the other dilutions: 1.0 as compared to 0.5. (Appendix B) This trend was observed for D8 normalization to all of the remaining housekeeping genes. (Appendix C) At the 0.05 dilution, a down-regulation of *Hox* D8 in sodium butyrate treated HT29 cells was observed, independently of the gene used for normalization. However, down-regulation folds differ depending on the reference gene and are higher when using the TBP gene that has a closer value to that of *Hox* D8.

Figure 6. (below) NaBT treated and untreated D8 expression after normalization to β-actin, ACTB, and TATA binding protein, TBP.

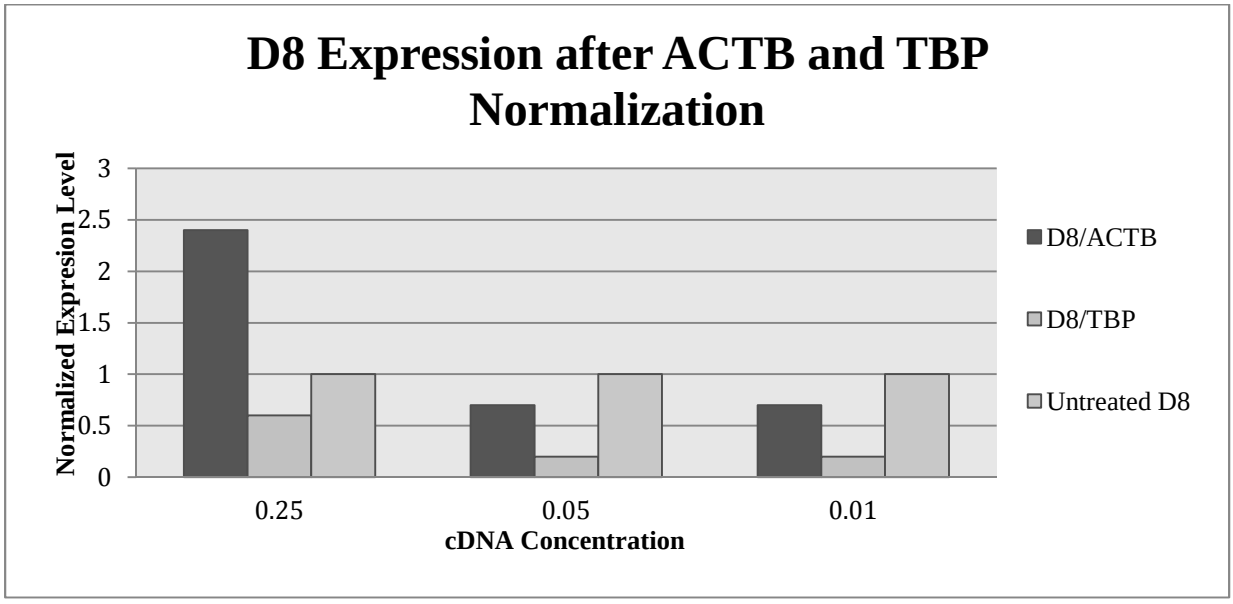

Figure 7. (below) NaBT treated and untreated D9 expression after normalization to β-actin, ACTB, and ribosomal protein L13a, RPL13a.

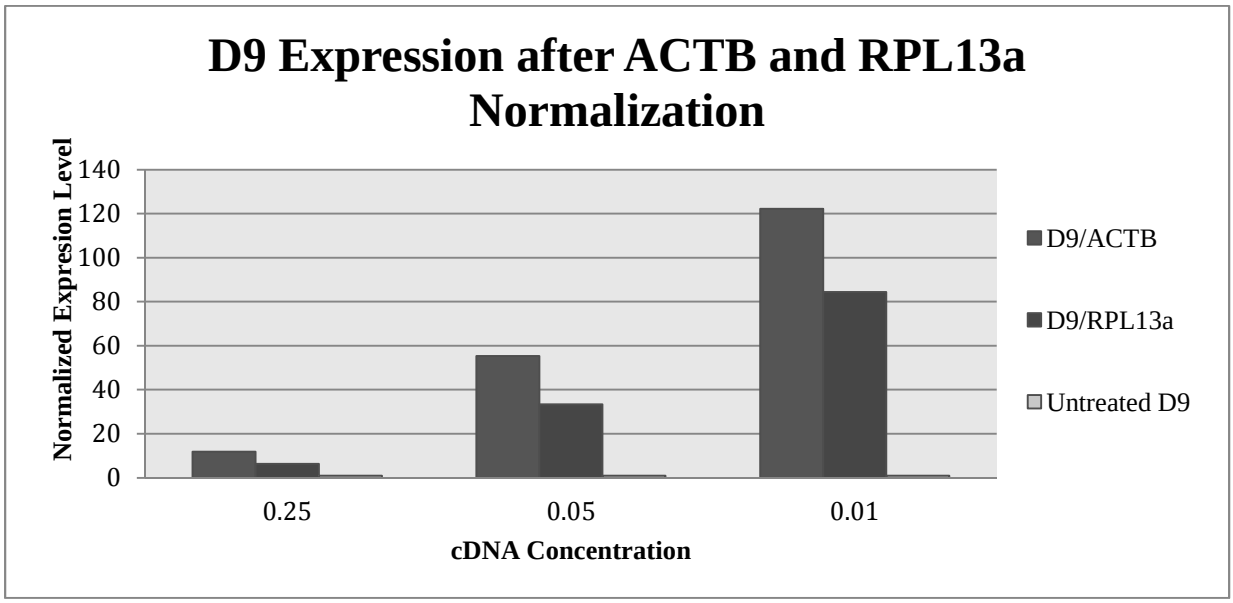

In Figure 7, D9 expression is normalized to ACTB and RPL13a. Because the C_T value for D9 was so much later than any of the others, both of the housekeeping genes differ in C_T. It can be determined from this figure that D9 has more variation within the samples for both treated ACTB and RPL13a. In addition, the level of expression indicates that in more dilute templates, there is a higher level of expression. Interestingly, the results showed an up-regulation of *Hox* D9, which contradict the observations from RT-PCR. The values for D9 can be accounted for by one of the following: 1) error propagation by incorrect efficiency calculations or 2) low detection and C_T values due to low levels of expression in the cells.

Overall, in *Hox* D8, the untreated HT29 had a higher level of expression than the 5 mM sodium butyrate treated HT29. *Hox* D9 had a higher level of expression in the treated HT29 versus the untreated HT29. (Appendix C)

3.3: *Hox* D8 and D9 Protein Expression

The third objective was to determine protein presence in the untreated and treated HT29 samples by use of Western blot and antibodies specific to *Hox* D8 and D9. If the Western blot validated the RT-PCR results, then expression of proteins D8 and D9 would be expected in untreated but not in NaBT treated HT29 cell lysates.

For both Western blots, three different sets of each untreated and treated cell lysates were used. The lanes were loaded as follows: 1- untreated 1, 2- treated 1, 3- untreated 2, and 4- treated 2. The loading control used was β-Actin, which is located at the bottom of the images. (Figure 8)

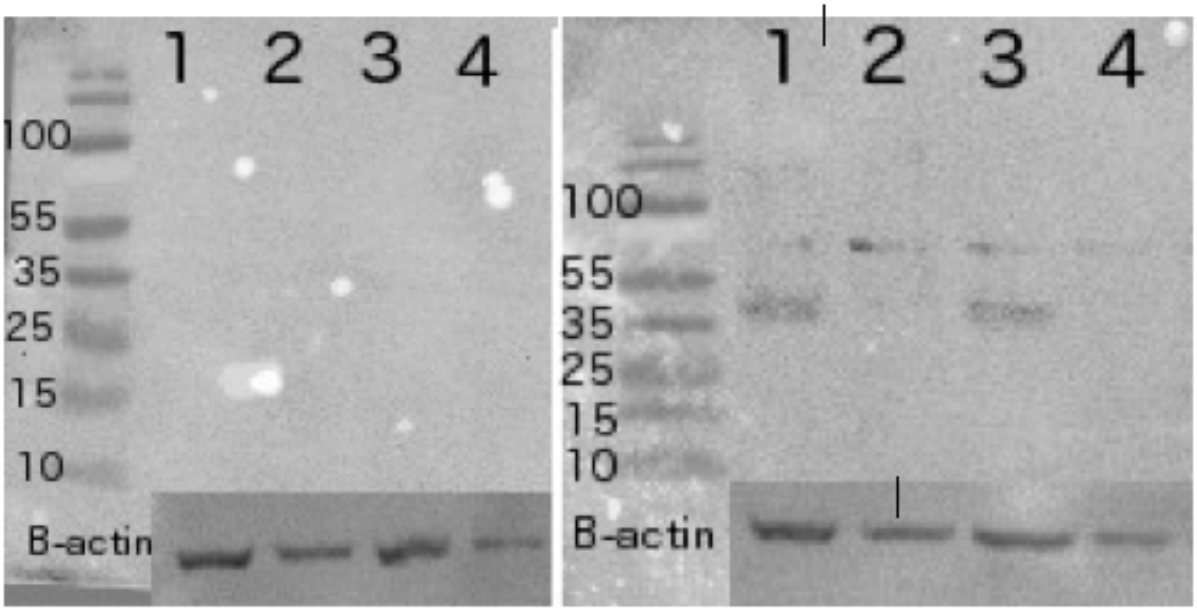

Figure 8. (above) Images of Western blot PVDF membranes for both *Hox* D8 (left) and D9 (right). Lanes for both correspond to the following: 1) Untreated Cell Lysate 1, 2) NaBT Treated Cell Lysate 1, 3) Untreated Cell Lysate 2, 4) NaBT Treated Cell Lysate 2. The size of the proteins: D8- 36.1 kDa, D9- 37 kDa, β-actin- 37 kDa. 10 µg of protein was loaded into each lane.

The size of the protein for *Hox* D8 was 36.1 kDa. (Novus Biologicals) The Western blot for this protein yielded no results as it either did not work under the conditions used, or there is no protein expression of *Hox* D8 in either untreated or treated HT29.

The size of the protein for *Hox* D9 was 37 kDa with a secondary unidentified protein located between 55 and 75 kDa. The protein was found to be expressed or present in untreated HT29 but not in the sodium butyrate treated HT29.

3.3: Ultrastructural Features of HT29 cells: Untreated and Sodium Butyrate Treated

In order to determine if sodium butyrate treatment had an effect on the phenotype of the treated cells when compared to untreated HT29 cells, the ultrastructure of both untreated and treated cells were studied with transmission electron microscopy. If sodium butyrate induced differentiation, the number of tight junctions and microvilli density should both increase as compared to the untreated HT29 cells. However, because HT29 in their “normal” or untreated state possess microvilli, tight junctions were identified and quantified.

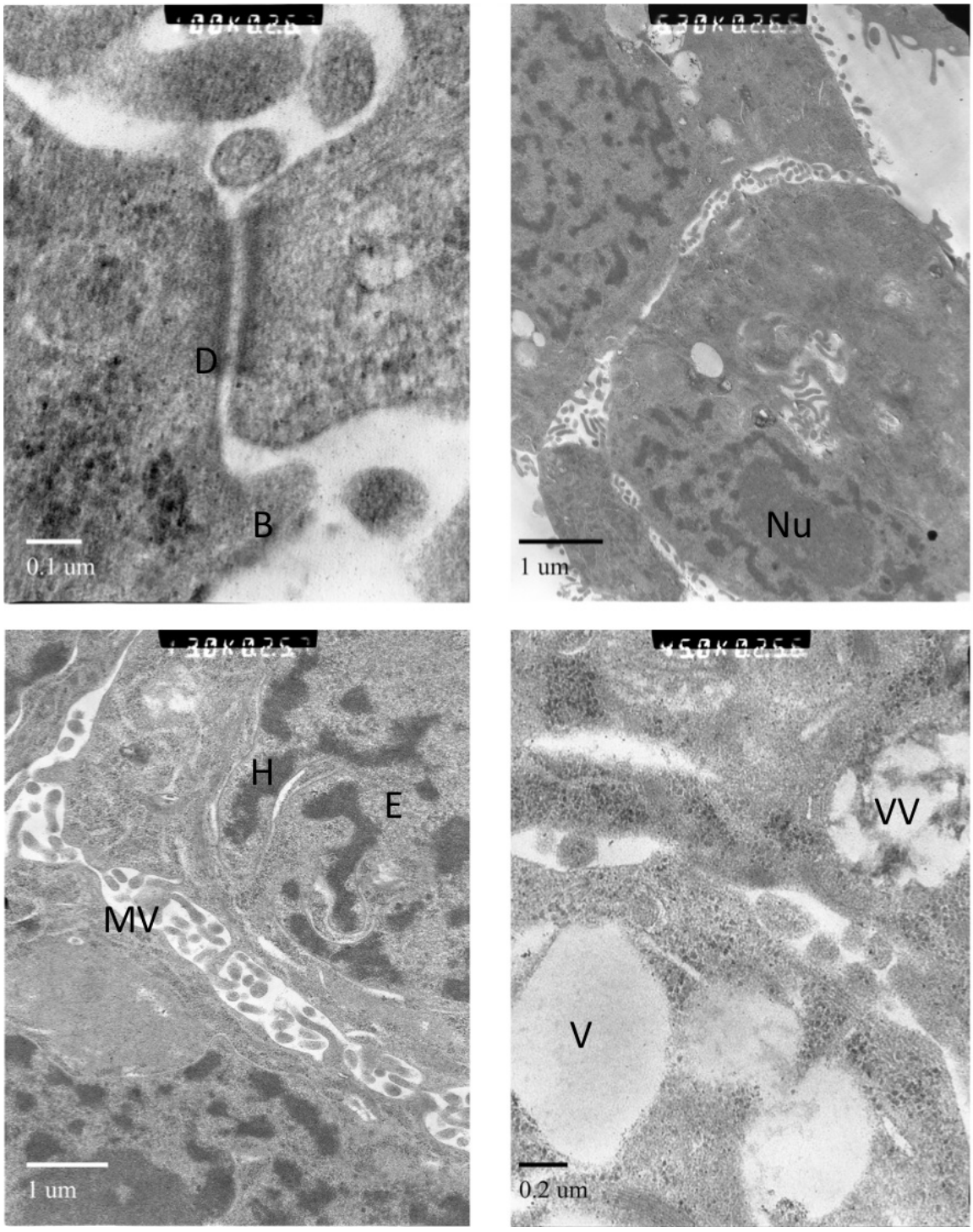

Figure 9. Micrographs of cellular junctions in untreated HT29. A- (100.0 x 10^3 magnification) A desmosome and a bleb protrusion. B- (6.3 x 10^3 magnification) Junctions at the convergence of three cells; the bottom left cell is in a different conformation potentially due to nonpolar, multi-layer growth. C- (13.0 x 10^3 magnification) The junction between two cells with a heavy concentration of microvilli in between. D- (45.0 x 10^3 magnification) A micrograph of a junction between two cells, containing vacuoles and vesicular vacuoles, as well as a desmosome. (B: Bleb, D: Desmosome, E: Euchromatin, H: Heterochromatin, MV: Microvilli, V: Vacuoles, VV: Vacuoles containing vesicles.)

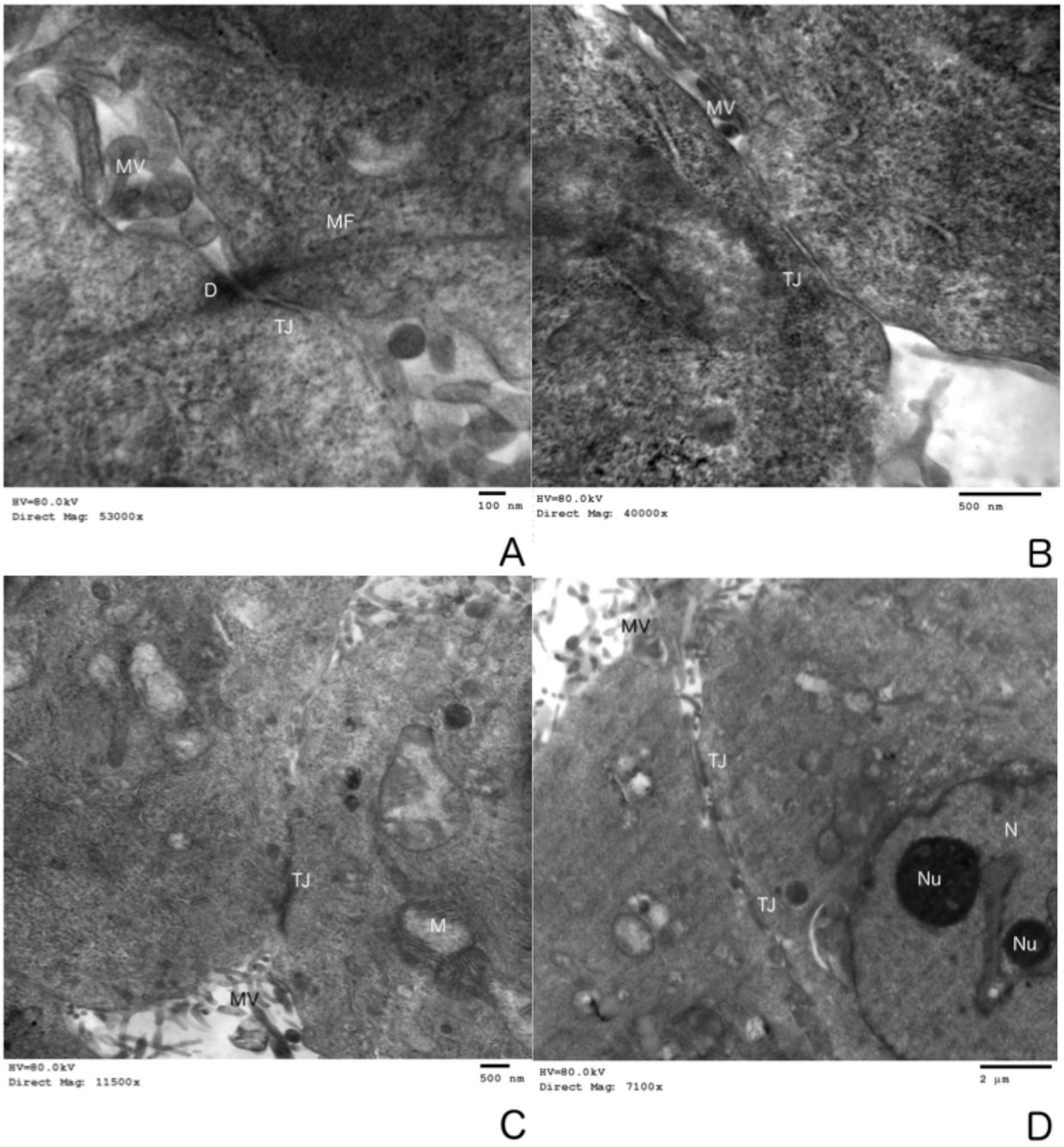

Figure 10. Micrographs of 5 mM NaBT treated HT29 cells. A- (53.0 x 10^3 magnification) A desmosome with its adjoining microfilaments and microvilli. B- (40.0 x 10^3 magnification) Tight junctions at the convergence of two cells, with some microvilli between the two cells . C- (11.5 x 10^3 magnification) A tight junction between two cells, with a mitochondria with well-defined cristae. D- (7.1 x 10^3 magnification) A micrograph of tight junctions between two cells, containing two nucleoli within the nucleus. (D: Desmosome, MV: Microvilli, N: Nucleus, Nu: Nucleolus.)

In both the untreated and treated HT29 cells, there was a high concentration of microvilli. (Appendix D) However, in terms of tight junctions between the cells, the number was much higher in 5 mM NaBT treated cells. In order to quantify this difference, the number of tight junctions at cellular interfaces was counted for each untreated and treated HT29 cell. For example, if there were two cells with a tight junction between them, a value of 1 was given for the tight junctions and a value of 2 was given to the cell number. In addition, there were desmosomes in both samples; they were quantified the same way as the cell number. As seen below in Table 7, the number of desmosomes and tight junctions increased in the treated HT29 cells in comparison with those of the untreated HT29.

Table 7. Quantification of the effects of sodium butyrate treatment on HT29 and the development of tight junctions and desmosomes. The number of desmosomes and tight junctions in both untreated and NaBT treated HT29 cells were counted for all of the cells imaged. The number represents the number of identifiable structures out of a total number or "cell count".

	Desmosomes	**Tight Junctions**	
	Number	Number	Cell Count
Untreated HT29	3	0	19
Sodium Butyrate Treated HT29	7	13	29

Tight junctions and desmosomes were identified as darkened or electron dense structures within the cells. Tight junctions are narrow and appear as a very defined membranous, "tube"-like structure at the interface between cells. Desmosomes have attached microfilaments that were seen going through the cell to the cellular interface and continuing on the other side. These structures are used for cellular adhesion.

The intracellular structures, cellular junctions, extracellular structures and general features of the cells were also studied. The cells range in size and shape dependent upon growth

conformation (i.e. multi-layered or monolayer) and orientation in the sections; however, the average cell size was approximately 8.5 μm in diameter. These cells have a high number of intracellular vacuoles, with some vacuoles containing vesicles. The vacuoles range in size from 0.50μm- 2.02μm in diameter. The vacuoles containing vesicles are somewhat intermediately sized around 1 μm in diameter. The HT29 cells show a nucleolus and a large amount of both heterochromatin and euchromatin (Figures 9-11, Appendix D) On average, the nucleoli had a diameter of 1.8 μm at the widest point. The size of the nucleus, at the widest point in diameter from membrane-membrane) is 4.8 μm on average. The cells also have microvilli projections from the membrane. The microvilli sizes range from 0.40 μm being the smallest, and 0.99 μm being the largest. Smaller projections, anything between 0.1-0.3 μm protrusions from the membrane are classified as blebs. These protrusions are extensions of the plasma membrane and are not considered members of the microvilli family.

In addition to the desmosomes, tight junctions and general features of the cells, there appeared to have been the formation of some type of apical domain in some of the cell sections of the sodium butyrate treated HT29. (Figure 11)

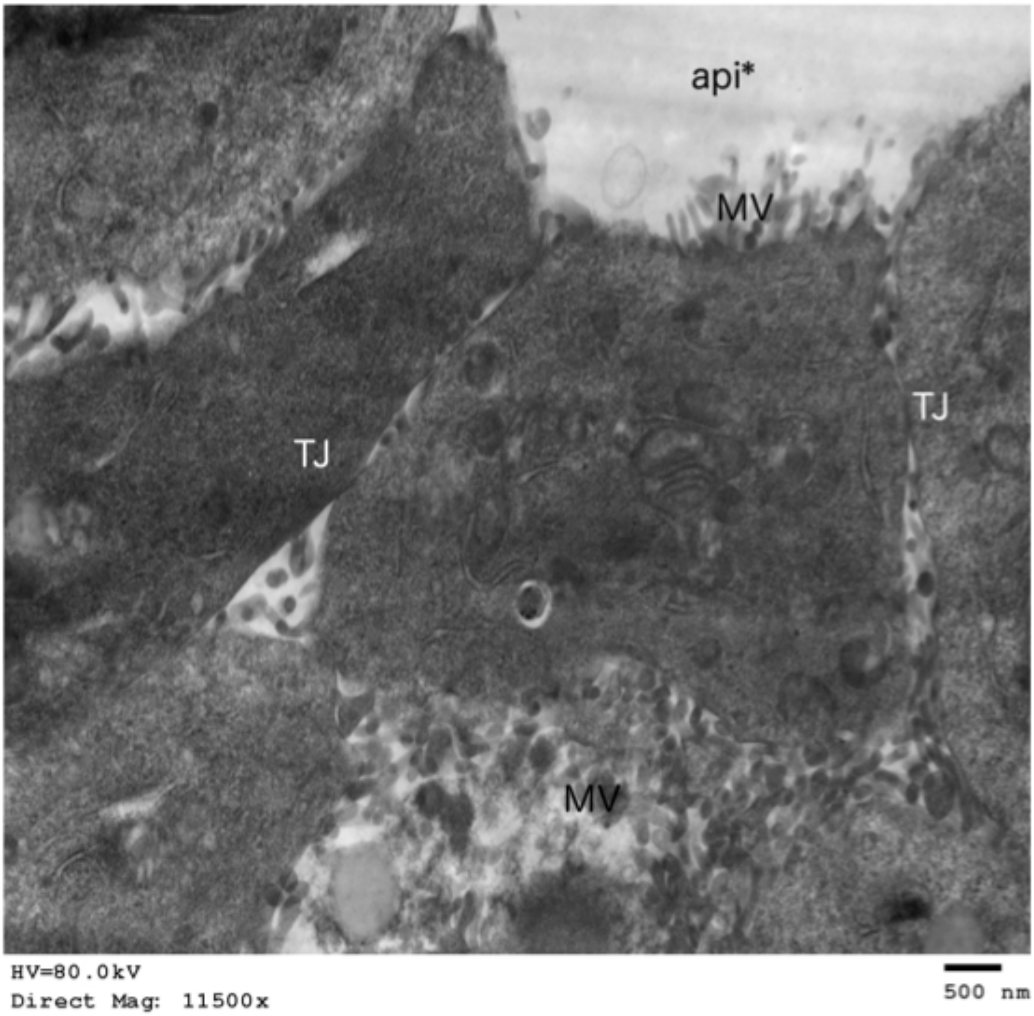

Figure 11. (11.5 x 10^3 magnification) 5 mM NaBT treated HT29 cells. In this micrograph, there appeared to be the formation of an apical (api*) domain at the top of the micrograph. The cells converged, possessing tight junctions (TJ) and microvilli (MV).

Chapter 4: Conclusions

In conclusion, the pattern of expression of *Hox* genes in untreated and treated HT29 cells led to suggest that D8 and D9 are responsible for maintaining the proliferative and undifferentiated state of the HT29 cells. This also suggests that sodium butyrate is inducing differentiation in this cell line. The findings provide some support to the original hypothesis that *Hox* genes expressed only in proliferating HT29 cells are responsible for maintaining the proliferative and undifferentiated state of these cells; however, the results remain too inconclusive to either accept or reject the hypothesis.

The targeted genes of interest, *Hox* D8 and D9, left some open-ended questions. The qRT-PCR results seemingly confirmed the observation of the RT-PCR experiments for gene D8. There was an increased level of expression in untreated cells, with a lower level of expression in the treated HT29 cells. However, there were some discrepancies with the resulting data for gene D9. There appeared to be a higher level of expression in treated than in untreated cells. This was not in agreement with the RT-PCR data where both genes were expected to have an up-regulated or higher level of expression in untreated versus treated. After reviewing the literature, there are some issues with the use of qRT-PCR to determine relative levels of gene expression. The problems arise with the interpretation of the results. Ideally, a target gene will be normalized to a stable internal control, or a reference gene that does not fluctuate in expression. When normalizing data against a housekeeping gene(s), variations can occur. For example, among different types of tissue, housekeeping genes can fluctuate in their level of expression. Additionally, if a treatment is used on cells in culture, the housekeeping gene expression can again be affected. [Vandesompele 2002] It is known that sodium butyrate has an effect on the

metabolism of cells, as well as other enzymes such as alkaline phosphatase. [Candido 1978] The housekeeping genes selected for this research have been used in other papers as reference genes for qRT-PCR; however, it is unknown if sodium butyrate treatment has any effect on their levels of expression. If these reference gene expression levels are being altered by treatment, using them as an internal control in these experiments could have propagated error in the data, as they are not truly stable.

The reference genes are not the only possible source of error in the resultant data for qRT-PCR. After treatment for seven days with sodium butyrate, it is assumed that all of the cells in culture have responded in the same way to the presence of the chemical. If sodium butyrate induces differentiation of HT29 cells, all of the cells present are differentiated, for example. It is known that the effects of sodium butyrate can be reversed if the chemical is no longer present in the culture media. Therefore, if the sodium butyrate was metabolized *in vitro* or was not at the appropriate concentration, the cells could begin to revert to an undifferentiated state. [Candido 1978]

Lastly, the error in D9 could be resultant of the gene being expressed at low level within the harvested cells. If the level of expression was beyond the sensitivity of detection in the reactions, the calculated values could in fact be erroneous.

In future research, a program such as geNorm (now part of the qBase+ software) should be used, in which the geometric mean of the output data for a battery of reference genes is normalized and the most stable of these genes is selected as the internal control for the genes of interest. Additionally, selecting reference genes that are not affected by sodium butyrate would be ideal. It could also be beneficial to design new sets of primers for the genes of interest. In

conclusion, because D8 seemed to confirm previous data and D9 did not, the results of qRT-PCR for these experiments may be unreliable data.

In analyzing the protein expression of *Hox* D8 and D9 by use of Western blot, it was observed that D9 was expressed only in untreated HT29 cell lysates. This confirmed the preliminary RT-PCR results. D8 did not have any protein expression in either untreated or treated cell lysates, which was unexpected from both RT- and qRT-PCR results. There are a few possible explanations for this occurring. First, it is possible that the conditions for the antibody although suggested by the company, were not optimal for the detection of protein. Or second, because there was expression of the gene in both RT- and qRT-PCR, mRNA is present in these cells but not being translated.

Additionally, there was a problem with the transfer, in which the lanes on the outermost side of the membranes did not transfer as well as the other lanes. This led to a less distinctive band in both the gene of interest (D9) and the β-actin loading control in lanes 5 and 6. The results in these lanes were in agreement with lanes 1-4. However, because of the slight decrease in intensity of the bands in the treated β-actin loading control versus the untreated controls; it brings into question whether the results of the Western are specific to the levels of D9 expression or are just an artifact of lower protein concentration in the samples.

Cell growth curves and transmission electron microscopy results suggest that sodium butyrate treatment is differentiating the cells. The ultrastructural phenotypes observed, such as the increase in tight junctions, desmosomes, potential apical domain and mucin granule formation; suggest that the cells begin to exhibit features of differentiated colonic epithelial cells.

This is reflected in the results of the cellular growth curve in which untreated HT29 cells are seen to exponentially proliferate while treated HT29 cells do not seem to grow.

These results are consistent with the literature. It has been observed that sodium butyrate acts to regulate cellular growth in many types of cells, most of which in a dose-dependent manner. [Van Wijk 1981] More specifically, research indicates that sodium butyrate inhibits proliferation and growth of HT29 cells *in vitro*. [Barnard 1993] The research conducted in sodium butyrate treated HT29 conclude that treatment inhibits cellular proliferation by inducing a block of cells at the G_0/G_1 phase of the cell cycle. [Barnard 1993, Coradini 2000] In one particular study of interest, cells were treated with sodium butyrate for three days at varying concentrations. The researchers observed 75% growth inhibition at a concentration of 4 mM sodium butyrate. They also noticed an increase in the percentage of cells with inhibited growth; a higher number of G_0/G_1 arrested cells, after an extended treatment period of 6 days. [Coradini 2000] The more recent studies indicate that at a higher concentration (4 mM and higher), cells first differentiate and eventually trigger apoptosis. [Barnard 1993, Coradini 2000] This cell cycle arrest is accompanied by metabolic changes in the cells, as well as histone deacetylase inhibitory activity. [Alcarraz-Vizián 2010]

In reviewing the literature to look for associations of the two genes of interest *Hox* D8 and D9 with proliferation of cells, it was recently reported that *Hox* genes of cluster D were expressed in neoplastic astrocytes and low-grade gliomas. [Abdel-Fattah 2006, Buccoliero 2009] Astrocytes are a type of glial cell, localized in the central nervous system. Gliomas are tumors of the brain and/or spinal cord. A low-grade glioma refers to the level of differentiation, much like in the colorectal adenocarcinoma cell line of study, which is moderately differentiated. This research led to further studies in which D9 expression was increased in stem cell-like gliomal

cells. Additionally, silencing the gene yielded apoptotic induction and lower expression of a cell-death regulating protein, Bcl-2. The researchers concluded that *Hox* D9 may promote survival of the cells and proliferation. [Tabuse 2011] Furthermore, D9 was also linked to a potential role in synoviocyte proliferation. Synoviocytes are fibroblast-like cells found in the synovial join of an organism. In this particular study, the cells were derived from patients with rheumatoid and osteo-arthritis. [Khoa 2001]

Because of the interest in the use of histone deacetylase inhibitors on tumorous metabolic pathways, and combined gene and drug therapies, future research could have vast implications. Any insight into the roles of specific genes and treatments on these cells in culture shed light on possible genes of interest to target for one of the leading causes of cancer-related death in the United States and western countries. [Alcarraz-Vizán 2010, CDC 2012, Coradini 2000] Future research could include further investigation of *Hox* genes D8 and D9, and the established objectives of this project. This includes analysis with a different type of software for qRT-PCR; with housekeeping genes that are identified as stable in both untreated and sodium butyrate treated HT29 cells. Additionally, conditions for *Hox* D8 Western blot could be optimized, or another antibody selected to verify the results of this research.

To ensure that the cells are effectively differentiated upon treatment with 5 mM sodium butyrate for seven days in culture, a dose-dependent cell growth curve and FACS analysis could be used. The dose-dependent response curve would indicate if cell proliferation inhibition was optimized at a 5 mM concentration. Flow cytometry or FACS analysis could be used to indicate if the results of the cell growth curve are due to the arrest of cells at the G_0/G_1 phase, as found in the literature.

To determine if the *Hox* genes D8 and D9 are responsible for maintaining the proliferative state of these cells, these genes could be targeted for silencing. Cell growth curves, FACS analysis, and q/RT-PCR detection of genes expressed only in a proliferating cell could be performed to determine if silencing inhibits cellular growth and proliferation. Additionally, other genes of the same paralogs could be tested for relative levels of expression upon silencing of the genes of interest. Recent research has also indicated that adjacent genes on the same cluster are more likely to have similar expression patterns than those located on different chromosomes. [Takahashi 2004] Therefore, genes in cluster D that also showed the differential pattern of expression could be targeted for further investigation.

APPENDIX A

Table 8. qRT-PCR data for each of the (7) housekeeping genes and (2) genes of interest. The cDNA dilution corresponds to the starting amount of template used for each reaction. The average C_T values were taken from all three trials and respective replicates. The efficiency calculated here is the average efficiency in both untreated and treated. These numbers were used for Pfaffl analysis of data.

	Gene	cDNA Dilution	Untreated Average C_T	Treated Average C_T	Average Efficiency
Housekeeping Reference Genes	**ACTB**	0.25	19.58	20.75	
		0.05	21.47	22.44	110.50%
		0.01	24.08	24.89	
	B2M	0.25	24.66	24.67	
		0.05	25.94	26.19	155.50%
		0.01	28.16	28.09	
	GAPDH	0.25	22.14	23.41	
		0.05	23.55	24.84	154.20%
		0.01	25.64	26.80	
	RPL13a	0.25	18.98	19.28	
		0.05	20.83	21.12	115.40%
		0.01	23.17	23.48	
	RPLPO	0.25	21.78	22.92	
		0.05	23.48	24.30	139.70%
		0.01	25.49	26.54	
	TBP	0.25	24.45	23.77	
		0.05	26.48	25.63	111.20%
		0.01	28.87	28.17	
	TFRC	0.25	24.80	24.46	
		0.05	26.81	26.31	105.80%
		0.01	29.36	28.82	
Hox Genes of Interest	**D8**	0.25	25.27	25.28	
		0.05	25.90	27.06	121.95%
		0.01	27.66	28.90	
	D9	0.25	33.80	32.28	
		0.05	37.44	34.33	188.26%
		0.01	38.53	34.56	

APPENDIX B

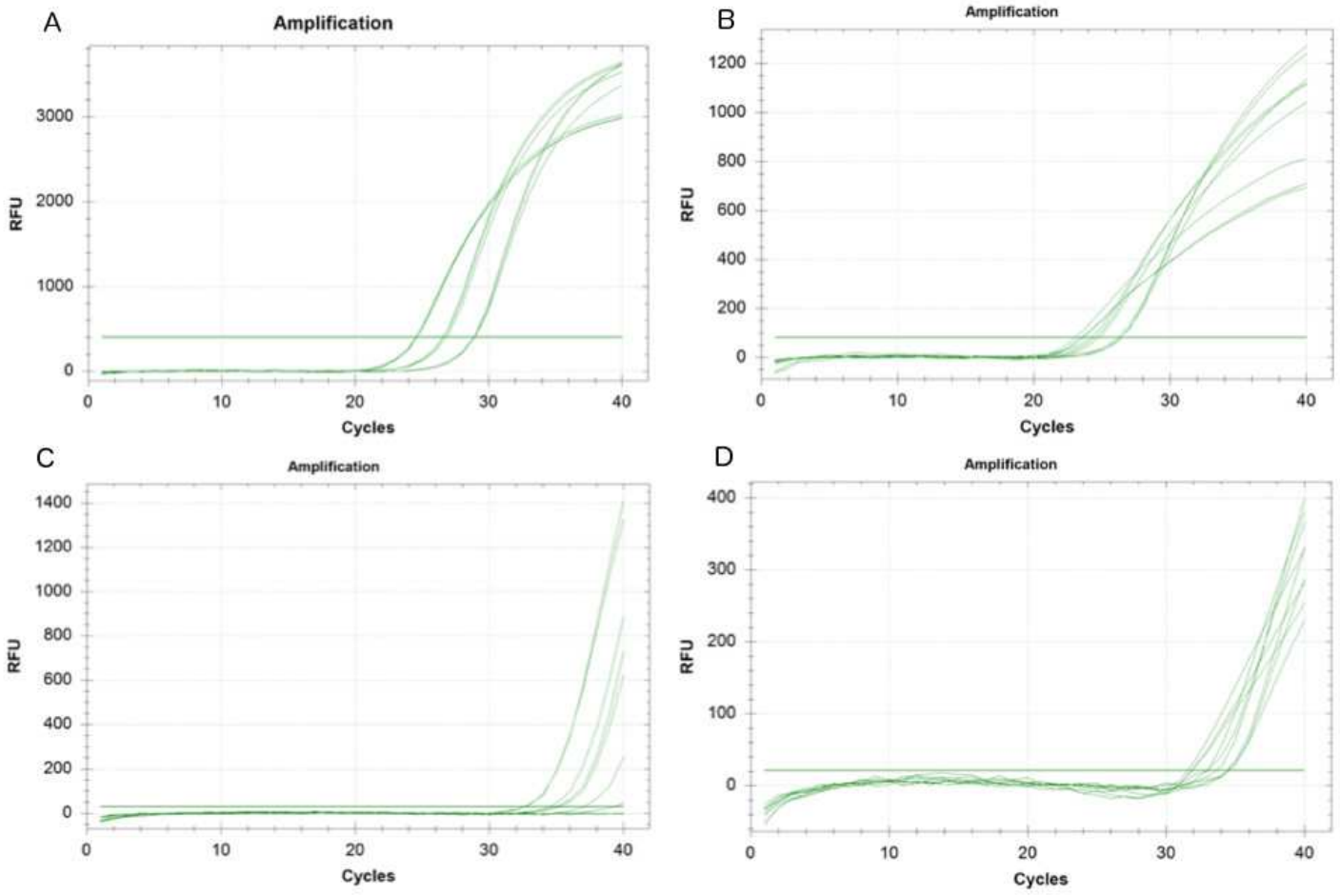

Figure 12. qRT-PCR raw data depicting relative fluorescence units (RFU) versus C_T for genes of interest D8 and D9. (A) Amplification curve for D8 in untreated HT29 cells. (B) Amplification curve for D8 in 5 mM sodium butyrate treated HT29 cells. (C) Amplification curve for D9 in untreated HT29 cells. (D) Amplification curve for D9 in 5 mM sodium butyrate treated HT29 cells.

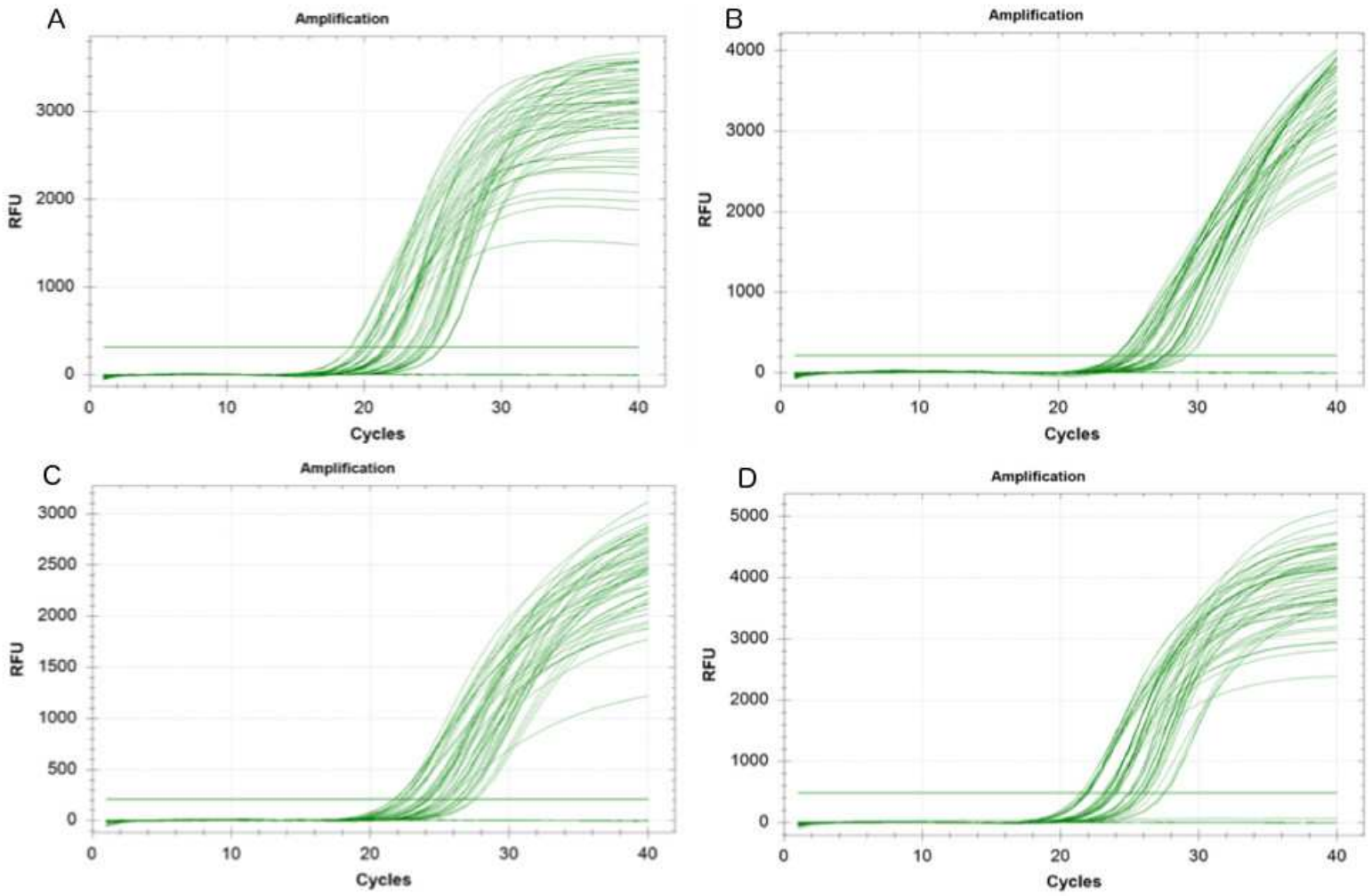

Figure 13. qRT-PCR raw data depicting relative fluorescence units (RFU) versus C_T for housekeeping genes ACTB, B2M, GAPDH and RPLPO. (A) Amplification curve for ACTB in both untreated and treated HT29 cells. (B) Amplification curve for B2M in both untreated and treated HT29 cells. (C) Amplification curve for GAPDH in both untreated and treated HT29 cells. (D) Amplification curve for RPLPO in both untreated and treated HT29 cells.

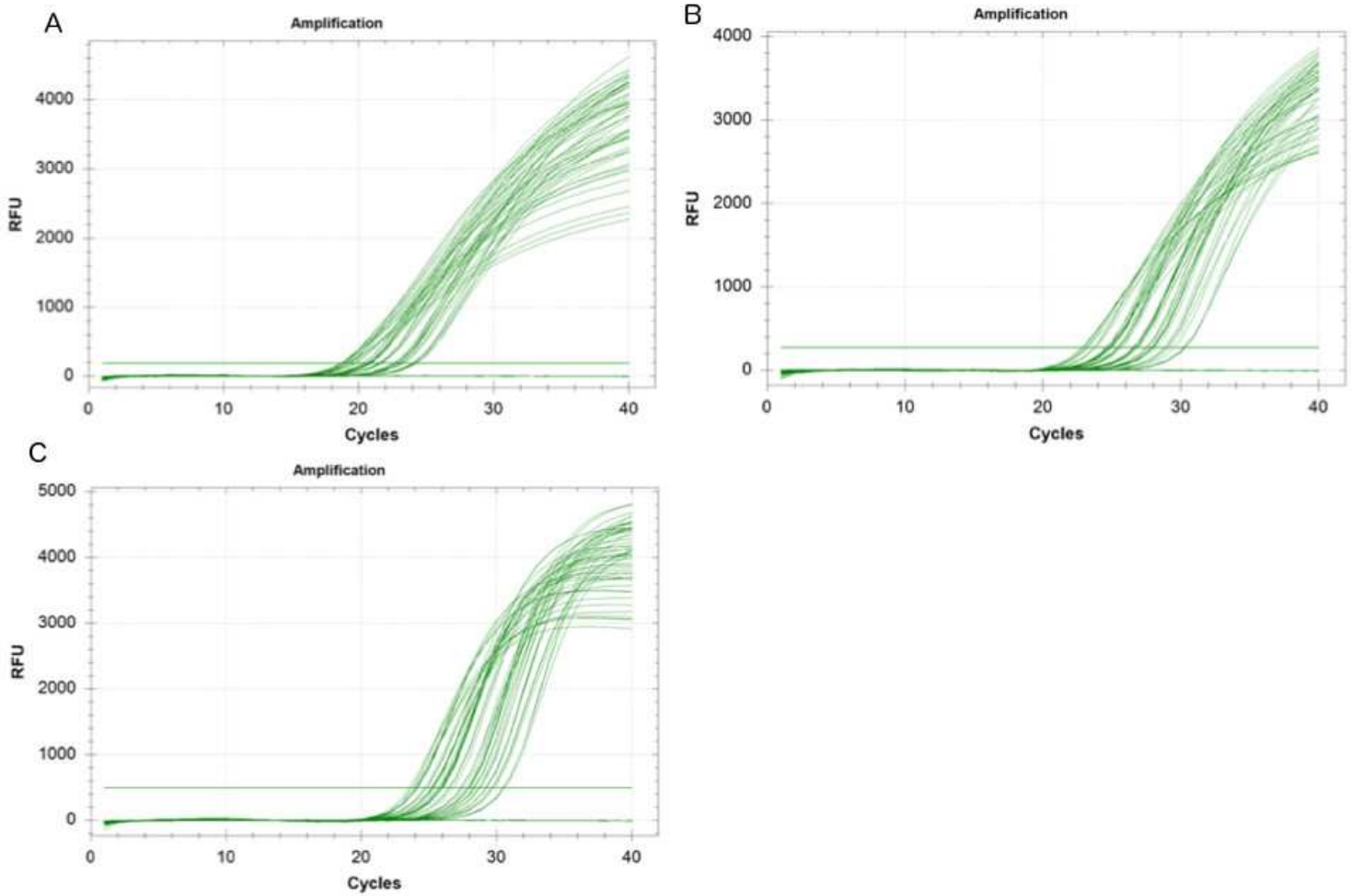

Figure 14. qRT-PCR raw data depicting relative fluorescence units (RFU) versus C_T for housekeeping genes RPL13a, TBP and TFRC. (A) Amplification curve for RPL13a in both untreated and treated HT29 cells. (B) Amplification curve for TBP in both untreated and treated HT29 cells. (C) Amplification curve for TFRC in both untreated and treated HT29 cells.

APPENDIX C

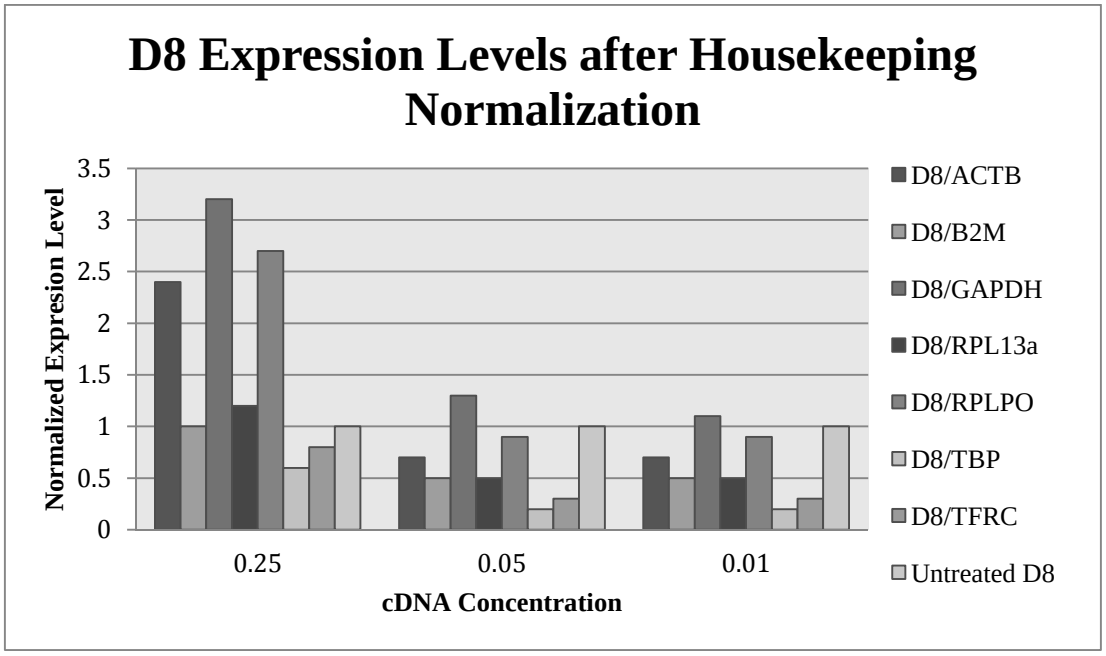

Figure 15. (above) Relative levels of expression of untreated and treated *Hox* D8 when normalized to each of the (7) housekeeping genes. A noticeable variation in the level of expression of D8 normalized to the housekeeping genes at a dilution of 0.25. However, the trend of a decreased level of expression of treated D8 compared to untreated D8 expression was observed for the other two dilutions.

Figure 16. (below) Relative levels of expression of untreated and treated *Hox* D9 when normalized to each of the (7) housekeeping genes. The trend of increased level of expression of housekeeping normalized treated D9 expression in comparison to untreated D9 was observed for all dilutions of the cDNA template.

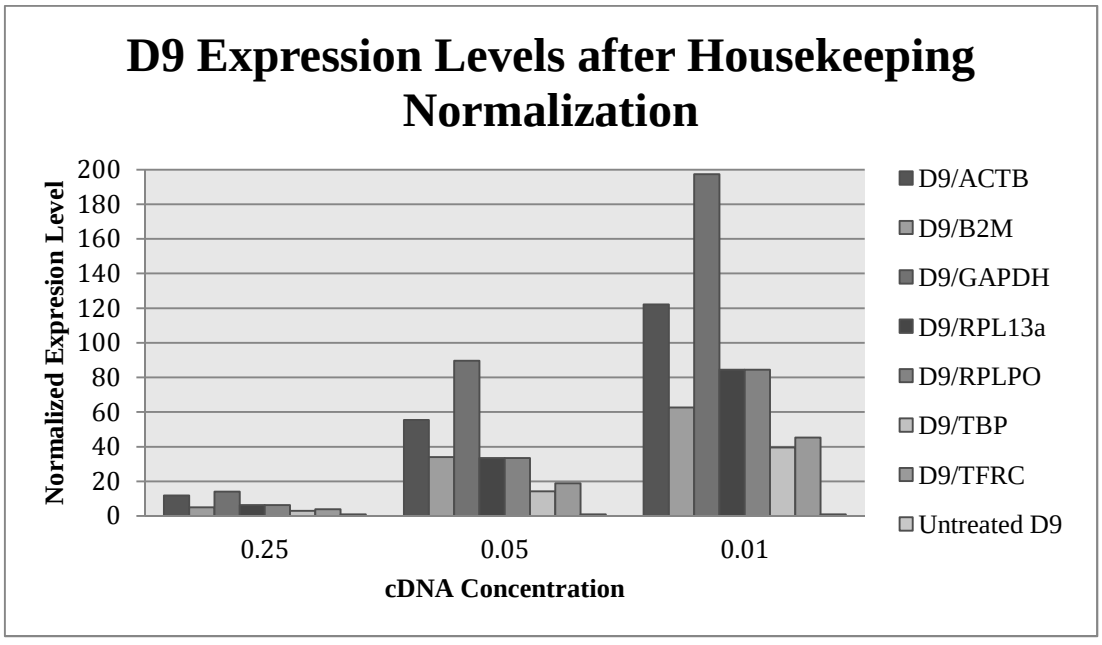

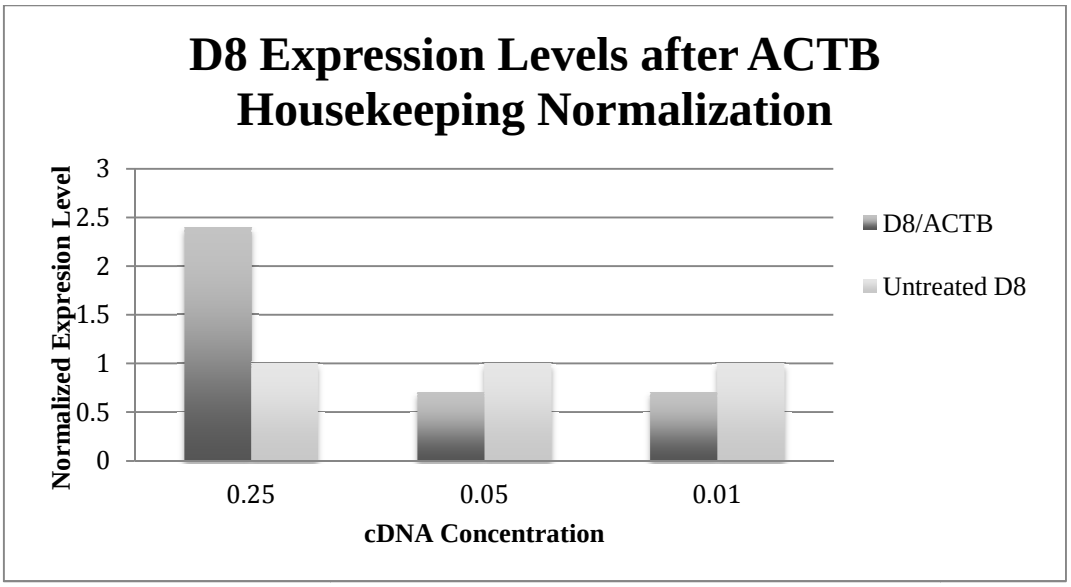

Figure 17. (above) Relative levels of expression of untreated and treated *Hox* D8 when normalized to housekeeping gene β-actin, ACTB. Treated D8 expression, normalized to ACTB, for each concentration of template was as follows (concentration = level of expression): 0.25 = 2.4, 0.05 = 0.7, and 0.01 = 0.7. The normalized value for untreated D8 = 1 at all concentrations.

Figure 18. (below) Relative levels of expression of untreated and treated *Hox* D8 when normalized to housekeeping gene β-2 microglobulin, B2M. Treated D8 expression, normalized to B2M, for each concentration of template was as follows (concentration = level of expression): 0.25 = 1.0, 0.05 = 0.5, and 0.01 = 0.5. The normalized value for untreated D8 = 1 at all concentrations.

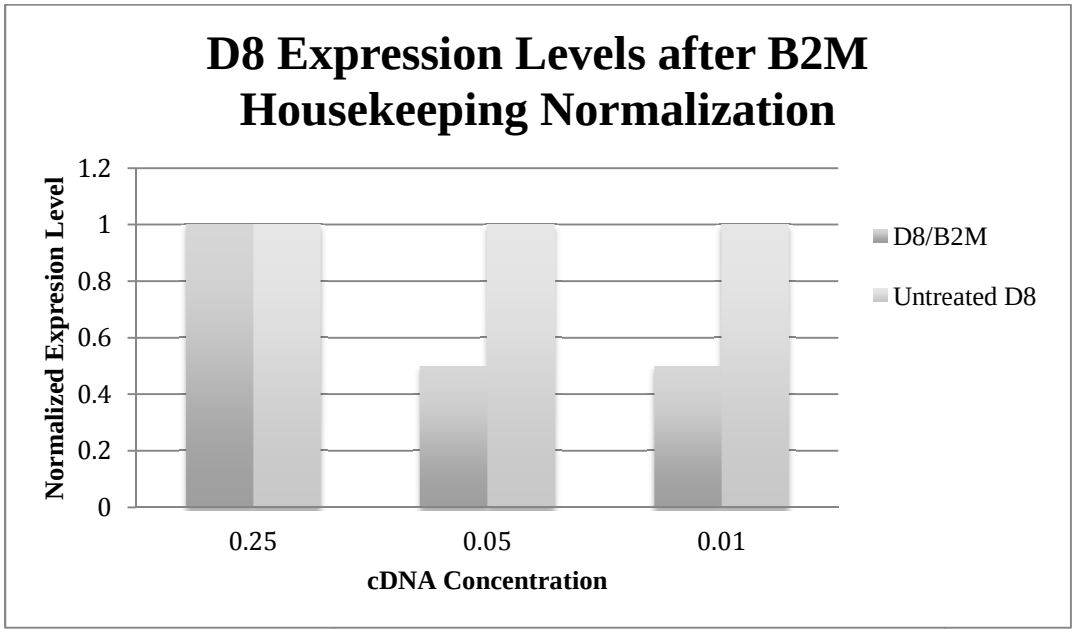

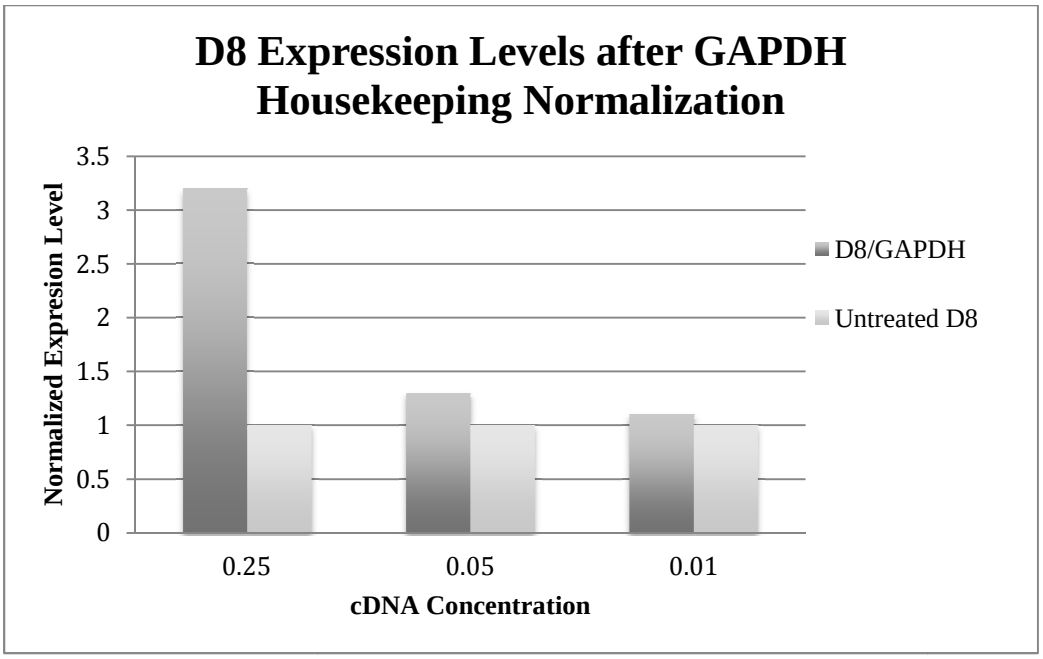

Figure 19. (above) Relative levels of expression of untreated and treated *Hox* D8 when normalized to housekeeping gene glyceradldehyde 3-phospate dehydrogenase, GAPDH. Treated D8 expression, normalized to GAPDH, for each concentration of template was as follows (concentration = level of expression): 0.25 = 3.2, 0.05 = 1.3, and 0.01 = 1.1. The normalized value for untreated D8 = 1 at all concentrations.

Figure 20. (below) Relative levels of expression of untreated and treated *Hox* D8 when normalized to housekeeping gene human acidic ribosomal protein 0, RPLPO. Treated D8 expression, normalized to RPLPO, for each concentration of template was as follows (concentration = level of expression): 0.25 = 2.7, 0.05 = 0.9, and 0.01 = 0.9. The normalized value for untreated D8 = 1 at all concentrations.

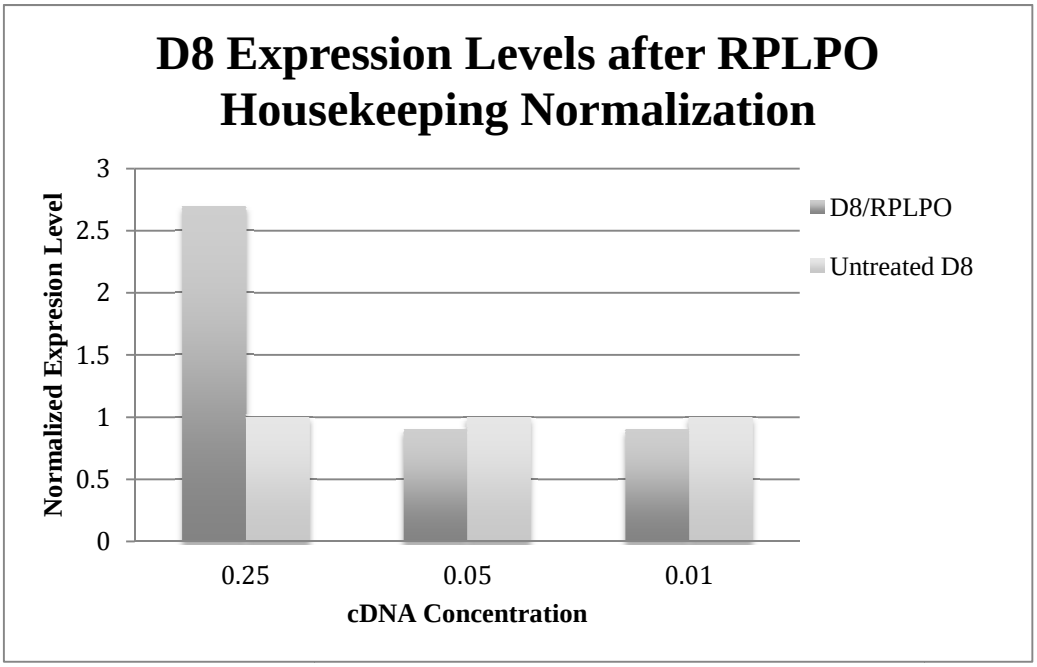

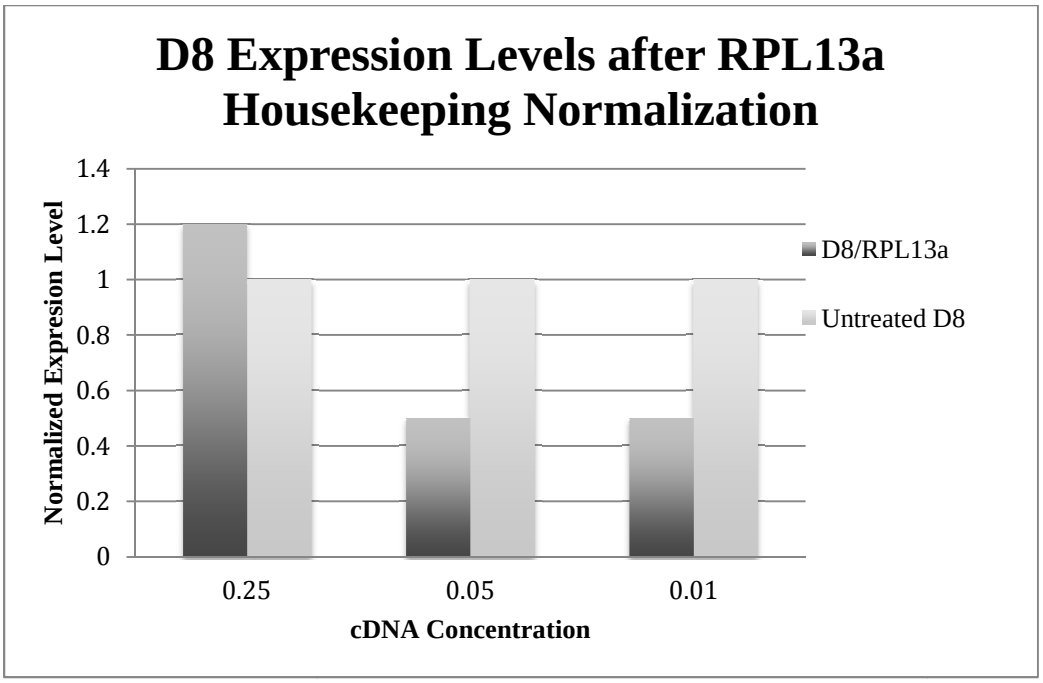

Figure 21. (above) Relative levels of expression of untreated and treated *Hox* D8 when normalized to housekeeping gene ribosomal protein L13a, RPL13a. Treated D8 expression, normalized to RPL13a, for each concentration of template was as follows (concentration = level of expression): 0.25 = 1.3, 0.05 = 0.5, and 0.01 = 0.5. The normalized value for untreated D8 = 1 at all concentrations.

Figure 22. (below) Relative levels of expression of untreated and treated *Hox* D8 when normalized to housekeeping gene TATA binding protein, TBP. Treated D8 expression, normalized to TBP, for each concentration of template was as follows (concentration = level of expression): 0.25 = 0.6, 0.05 = 0.2, and 0.01 = 0.2. The normalized value for untreated D8 = 1 at all concentrations.

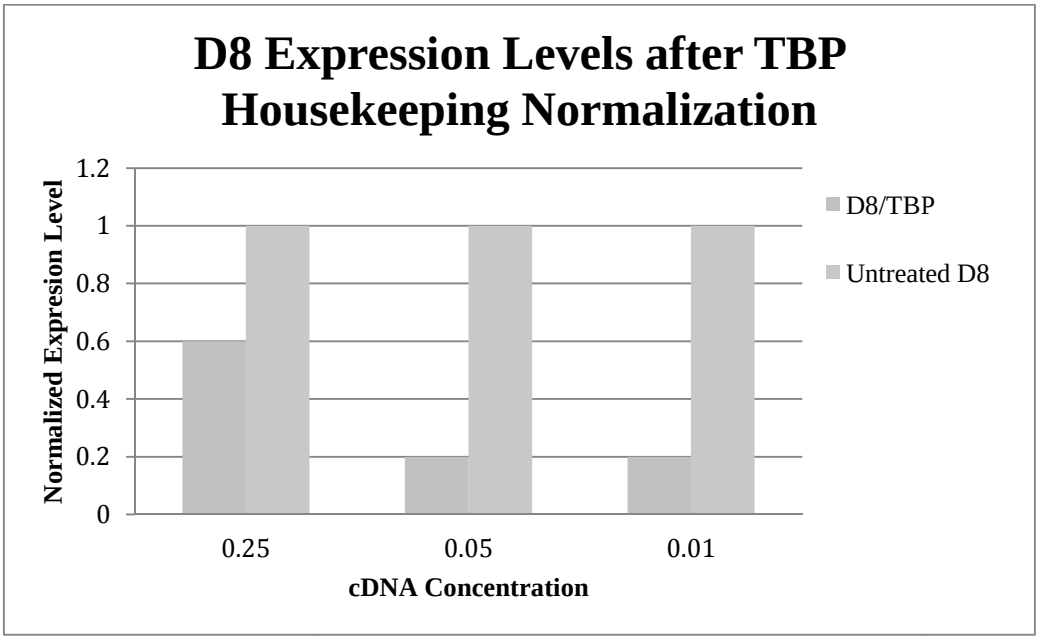

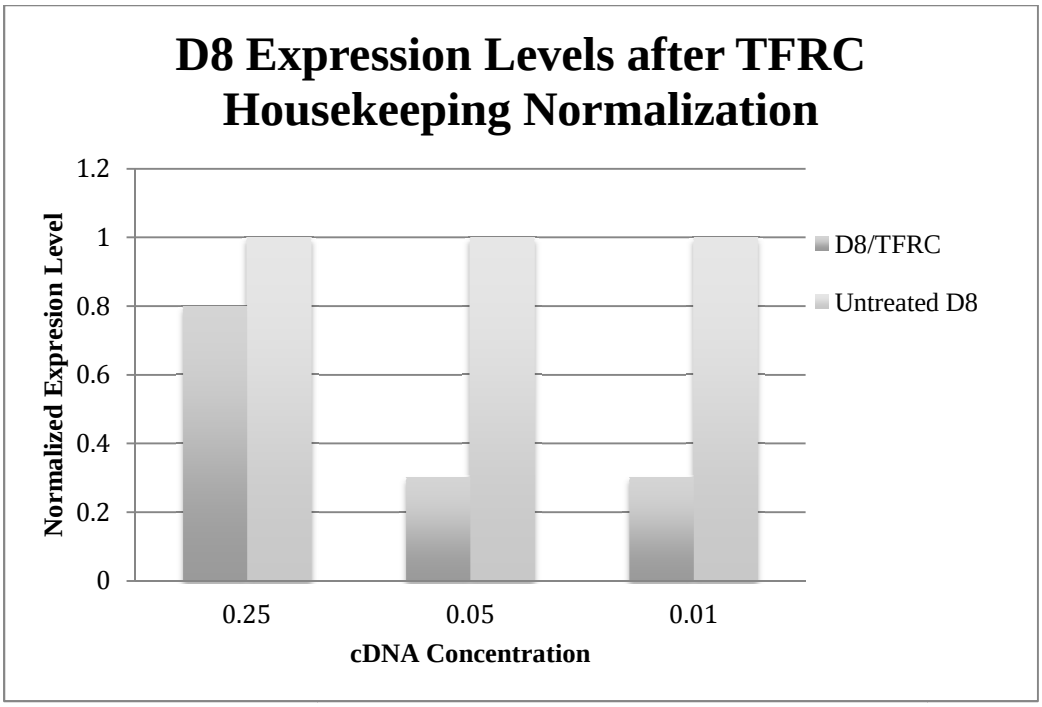

Figure 23. (above) Relative levels of expression of untreated and treated *Hox* D8 when normalized to housekeeping gene transferrin receptor C, TFRC. Treated D8 expression, normalized to TFRC, for each concentration of template was as follows (concentration = level of expression): 0.25 = 0.8, 0.05 = 0.3, and 0.01 = 0.3. The normalized value for untreated D8 = 1 at all concentrations.

Figure 24. (below) Relative levels of expression of untreated and treated *Hox* D9 when normalized to housekeeping gene β-Actin, ACTB. Treated D8 expression, normalized to ACTB, for each concentration of template was as follows (concentration = level of expression): 0.25 = 11.9, 0.05 = 55.4, and 0.01 = 122.2. The normalized value for untreated D8 = 1 at all concentrations.

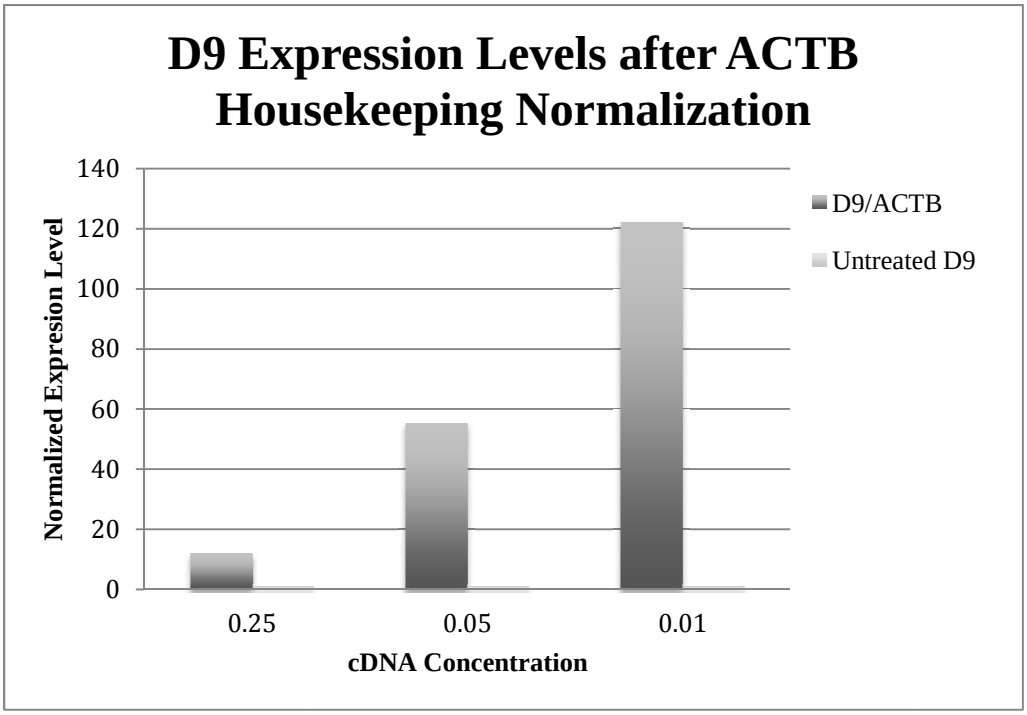

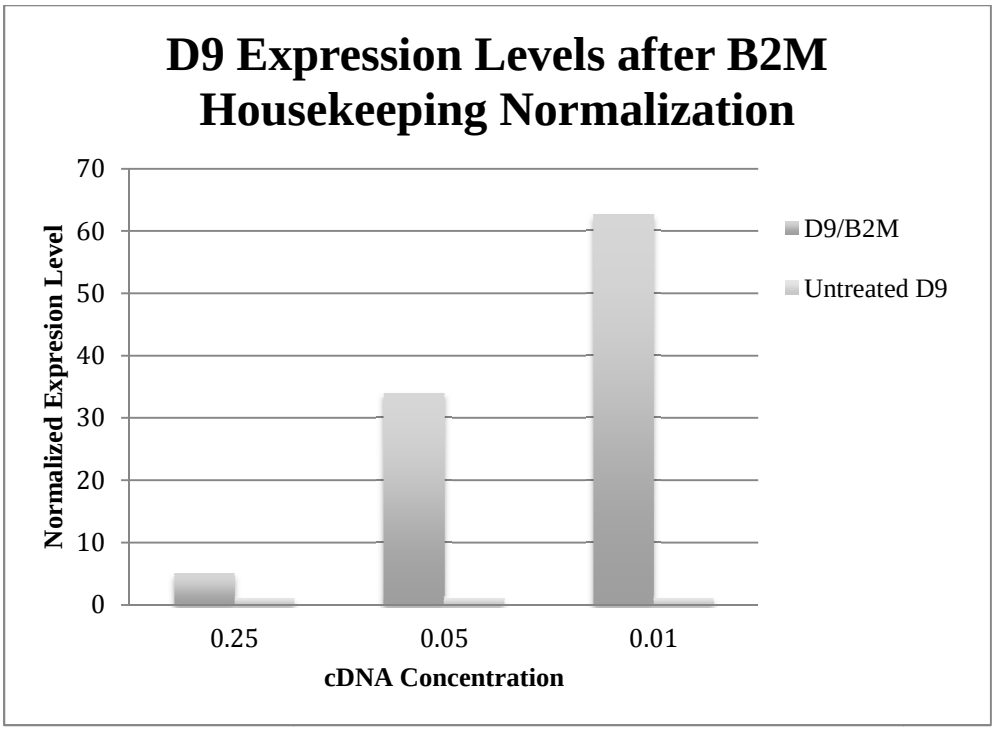

Figure 25. (above) Relative levels of expression of untreated and treated *Hox* D9 when normalized to housekeeping gene β-2 microglobulin, B2M. Treated D8 expression, normalized to B2M, for each concentration of template was as follows (concentration = level of expression): 0.25 = 5.0, 0.05 = 34.0, and 0.01 = 62.6. The normalized value for untreated D8 = 1 at all concentrations.

Figure 26. (below) Relative levels of expression of untreated and treated *Hox* D9 when normalized to housekeeping gene glyceraldehyde 3-phospate dehydrogenase, GAPDH. Treated D8 expression, normalized to GAPDH, for each concentration of template was as follows (concentration = level of expression): 0.25 = 14.1, 0.05 = 89.7, and 0.01 = 197.4. The normalized value for untreated D8 = 1 at all concentrations.

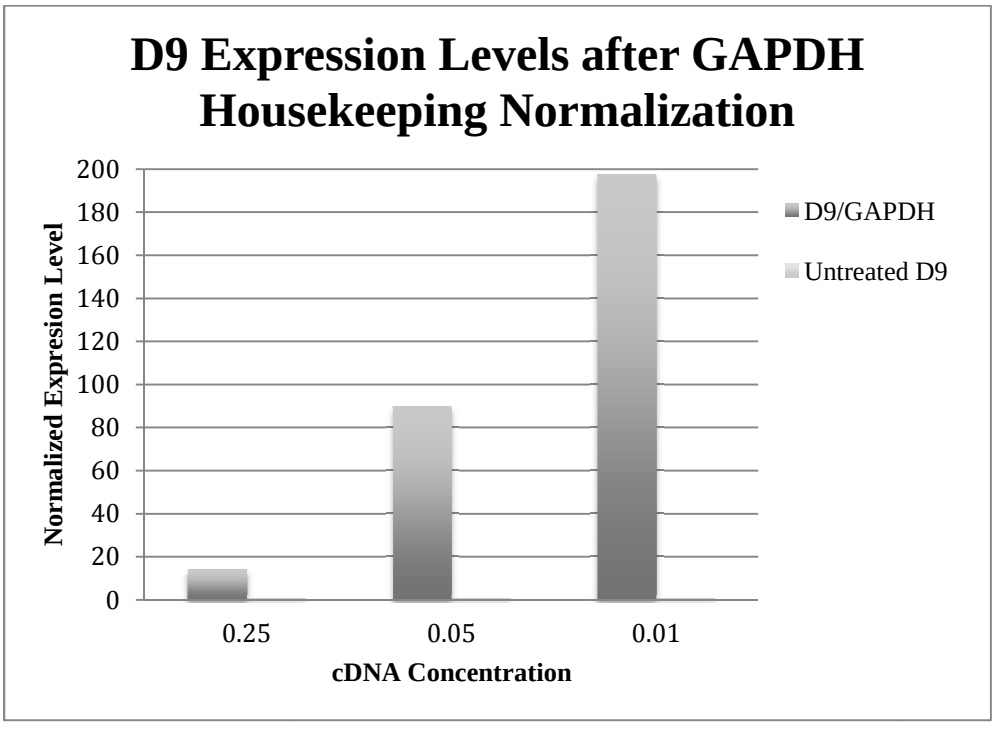

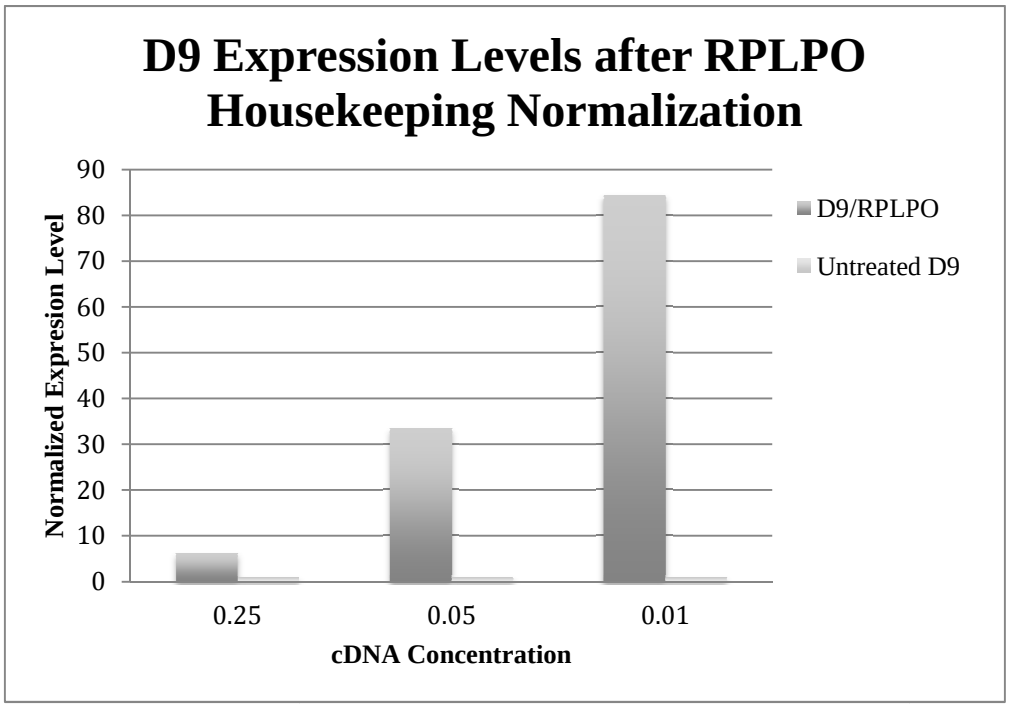

Figure 27. (above) Relative levels of expression of untreated and treated *Hox* D9 when normalized to housekeeping gene human acidic ribosomal protein 0, RPLPO. Treated D8 expression, normalized to RPLPO, for each concentration of template was as follows (concentration = level of expression): 0.25 = 13.5, 0.05 = 55.1, and 0.01 = 167.5. The normalized value for untreated D8 = 1 at all concentrations.

Figure 28. (below) Relative levels of expression of untreated and treated *Hox* D9 when normalized to housekeeping gene ribosomal protein L13a, RPL13a. Treated D8 expression, normalized to RPL13a, for each concentration of template was as follows (concentration = level of expression): 0.25 = 6.3, 0.05 = 33.4, and 0.01 = 84.4. The normalized value for untreated D8 = 1 at all concentrations.

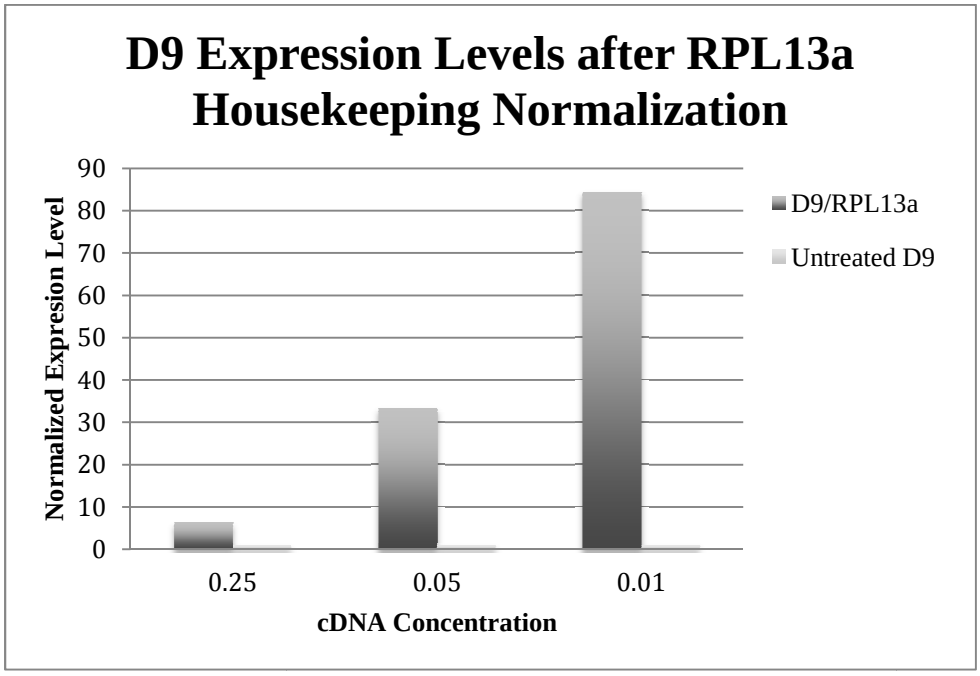

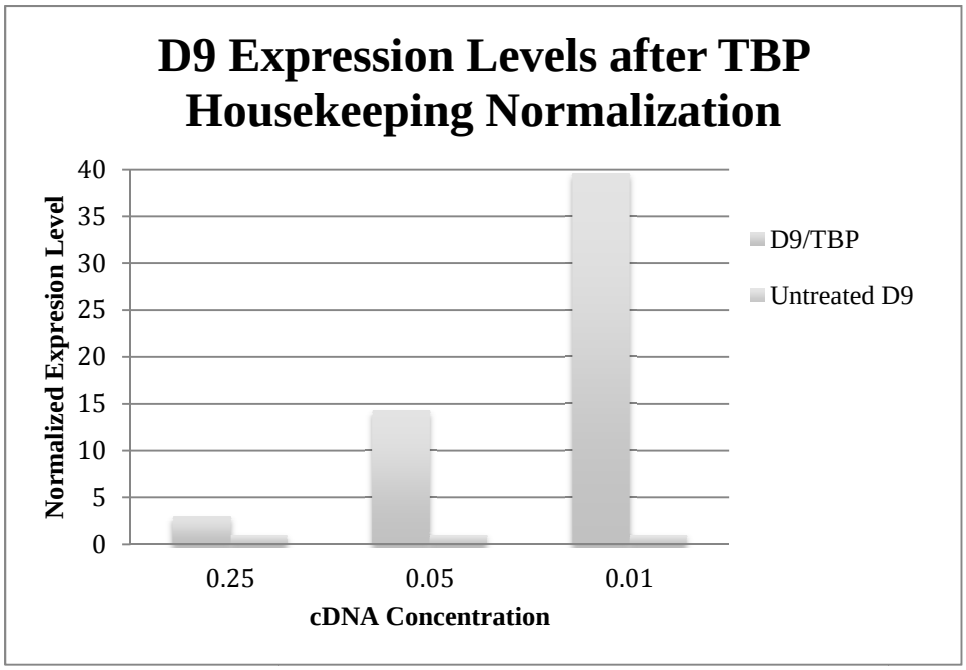

Figure 29. Relative levels of expression of untreated and treated *Hox* D9 when normalized to housekeeping gene TATA binding protein, TBP. Treated D8 expression, normalized to TBP, for each concentration of template was as follows (concentration = level of expression): 0.25 = 3.0, 0.05 = 14.3, and 0.01 = 39.6. The normalized value for untreated D8 = 1 at all concentrations.

Figure 30. Relative levels of expression of untreated and treated *Hox* D9 when normalized to housekeeping gene transferrin receptor C, TFRC. Treated D8 expression, normalized to TFRC, for each concentration of template was as follows (concentration = level of expression): 0.25 = 3.9, 0.05 = 18.8, and 0.01 = 45.3. The normalized value for untreated D8 = 1 at all concentrations.

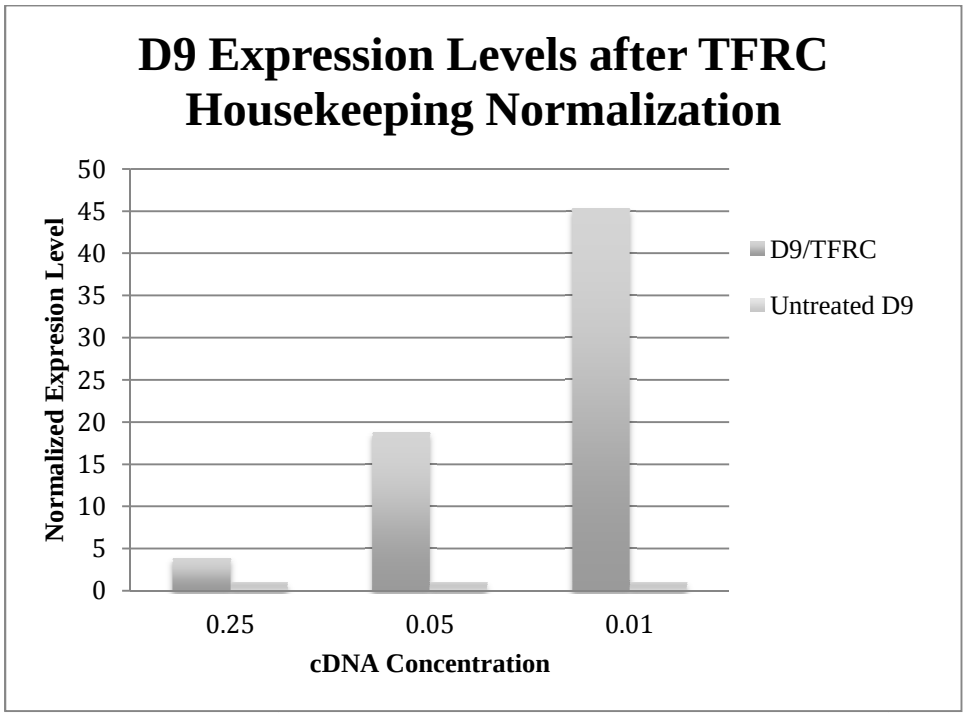

APPENDIX D

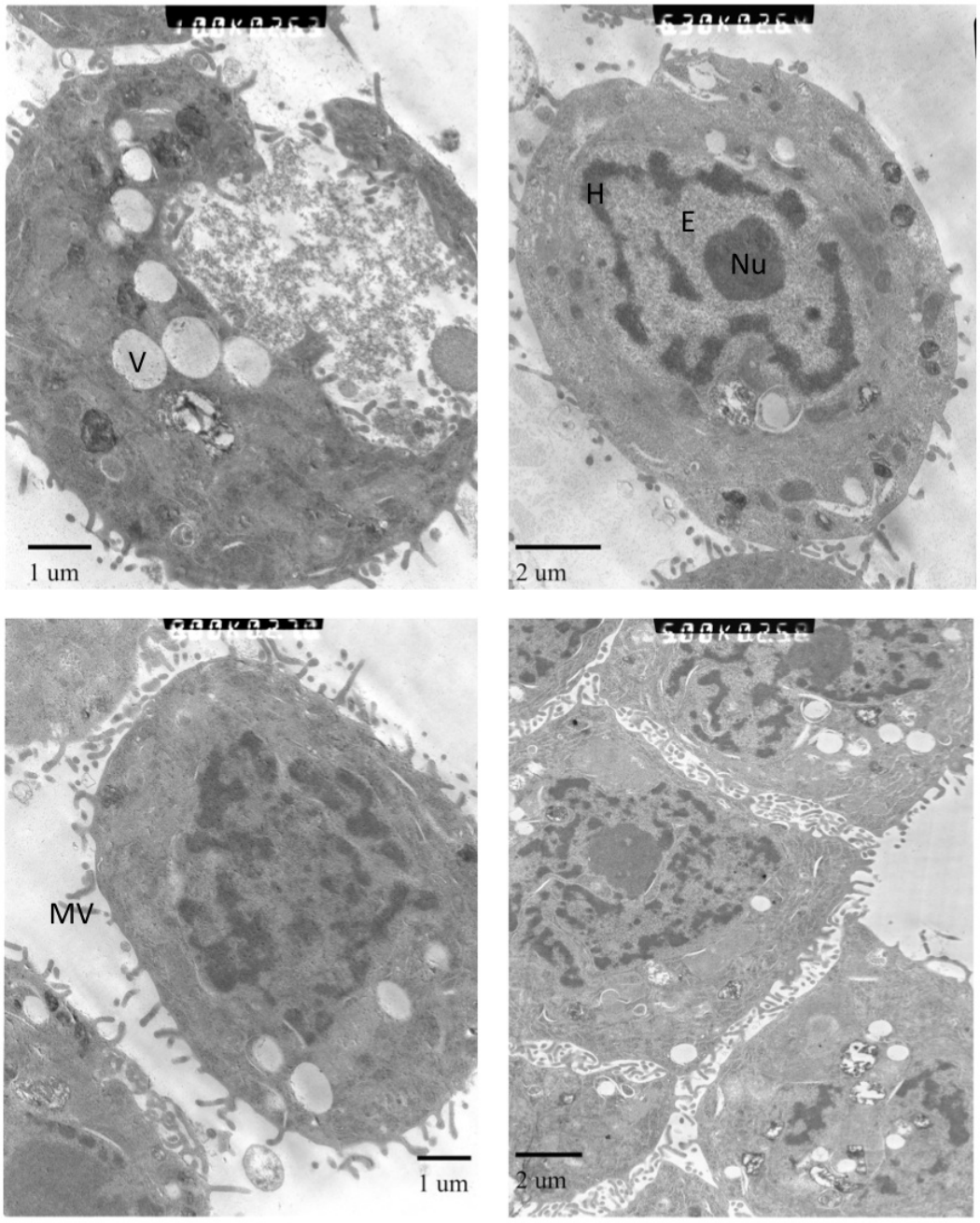

Figure 31. Transmission electron micrographs analyzing at the general features of untreated HT29 cells. A- (10.0 x 10^3 magnification) HT29 cell undergoing lysis. B- (6.3 x 10^3 magnification) entire HT29 cell. C- (8.0 x 10^3 magnification) cell near a junction with another. D- (5.0 x 10^3 magnification) convergence of 5 HT29 cells and the junctions between them, with high concentrations of microvilli. The shape amongst these cells is attributed to nonpolar, multi-layer growth. (E: Euchromatin, H: Heterochromatin, MV: Microvilli, Nu: Nucleolus, V: Vacuole)

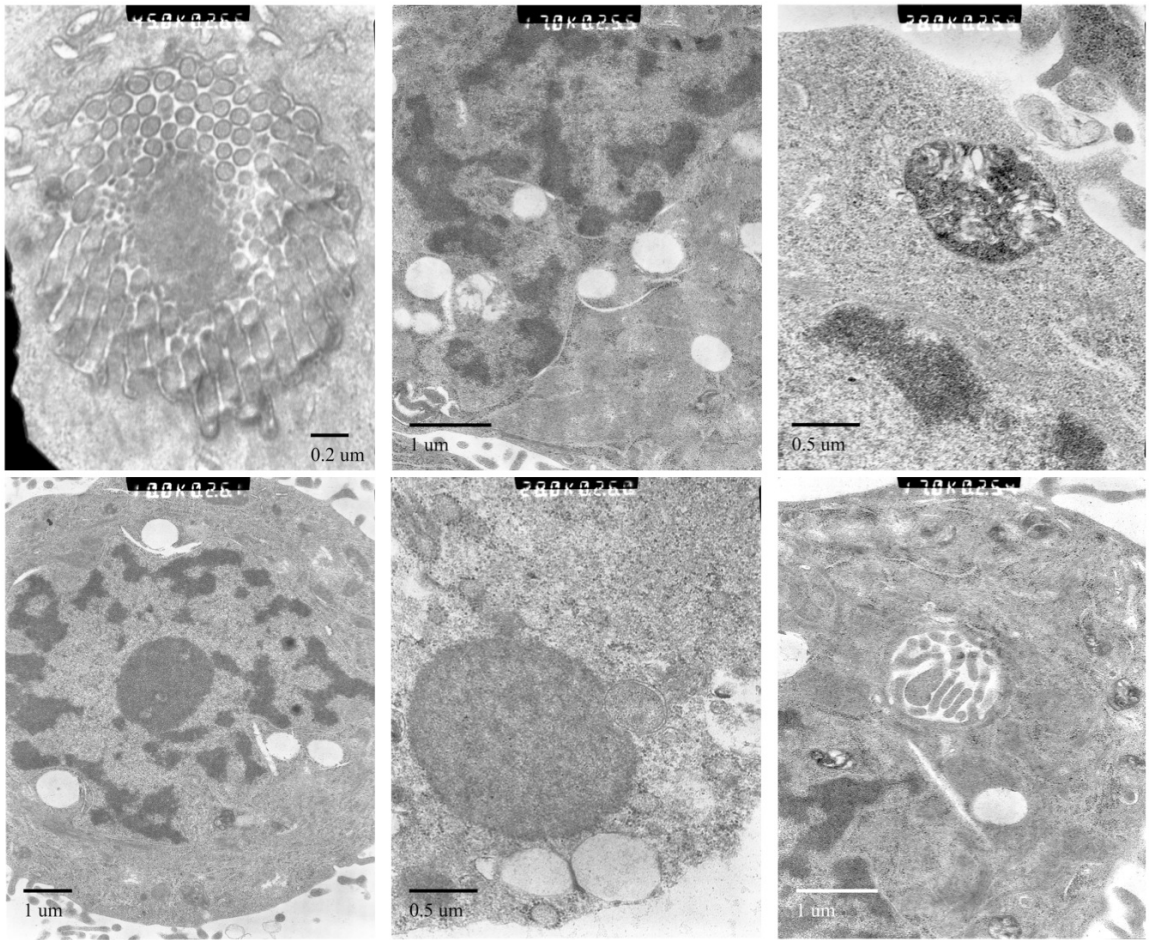

Figure 32. Micrographs of various intracellular structures and organelles within untreated HT29 cells. A- 45.0 x 10^3 magnification micrograph of a cell conformation with microvilli. B- 17.0 x 10^3 magnification micrograph of intracellular vacuoles both with and without vesicles, and heterochromatin. C- 28.0 x 10^3 magnification micrograph of what appears to be a mitochondria near the outside of the cell. D- 10.0 x 10^3 of a cell, nucleolus, vacuoles, heterochromatin and euchromatin. E- 28.0 x 10^3 magnification micrograph of a nucleolus and membrane bound organelle. F- 17.0 x 10^3 magnification micrograph of a structure similar to that in (A).

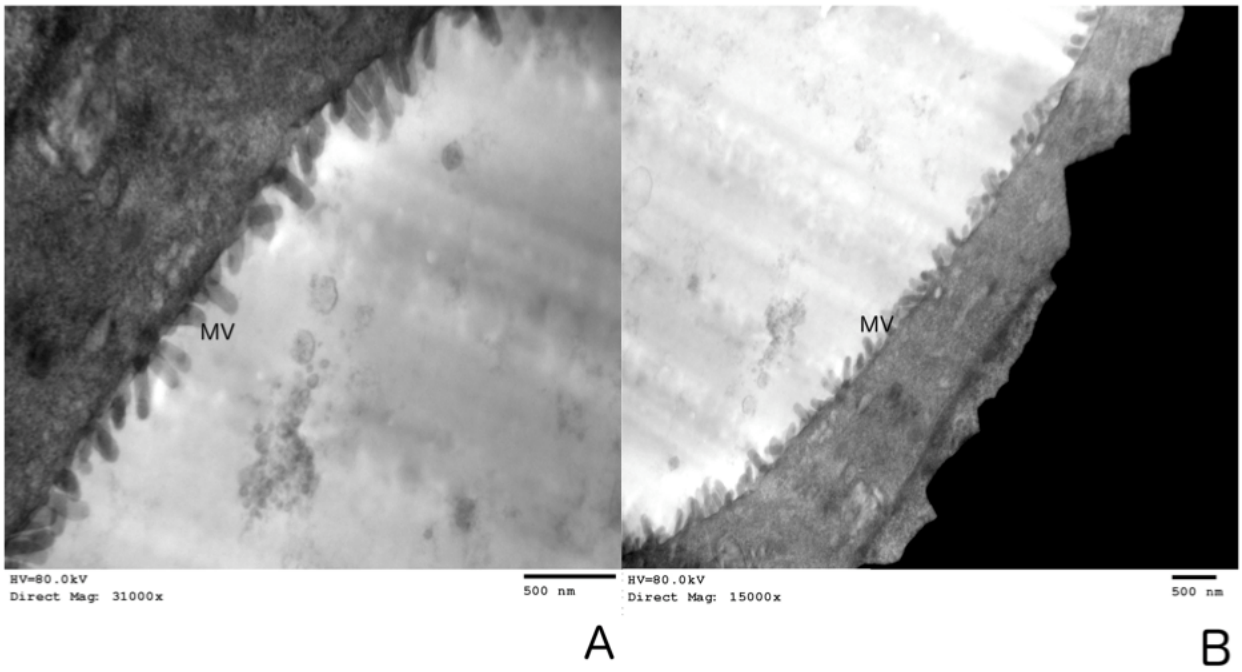

Figure 33. Micrographs of microvilli in 5 mM NaBT treated HT29 cells. A- 31.0 x 10^3 magnification. B- 15.0 x 10^3 magnification.

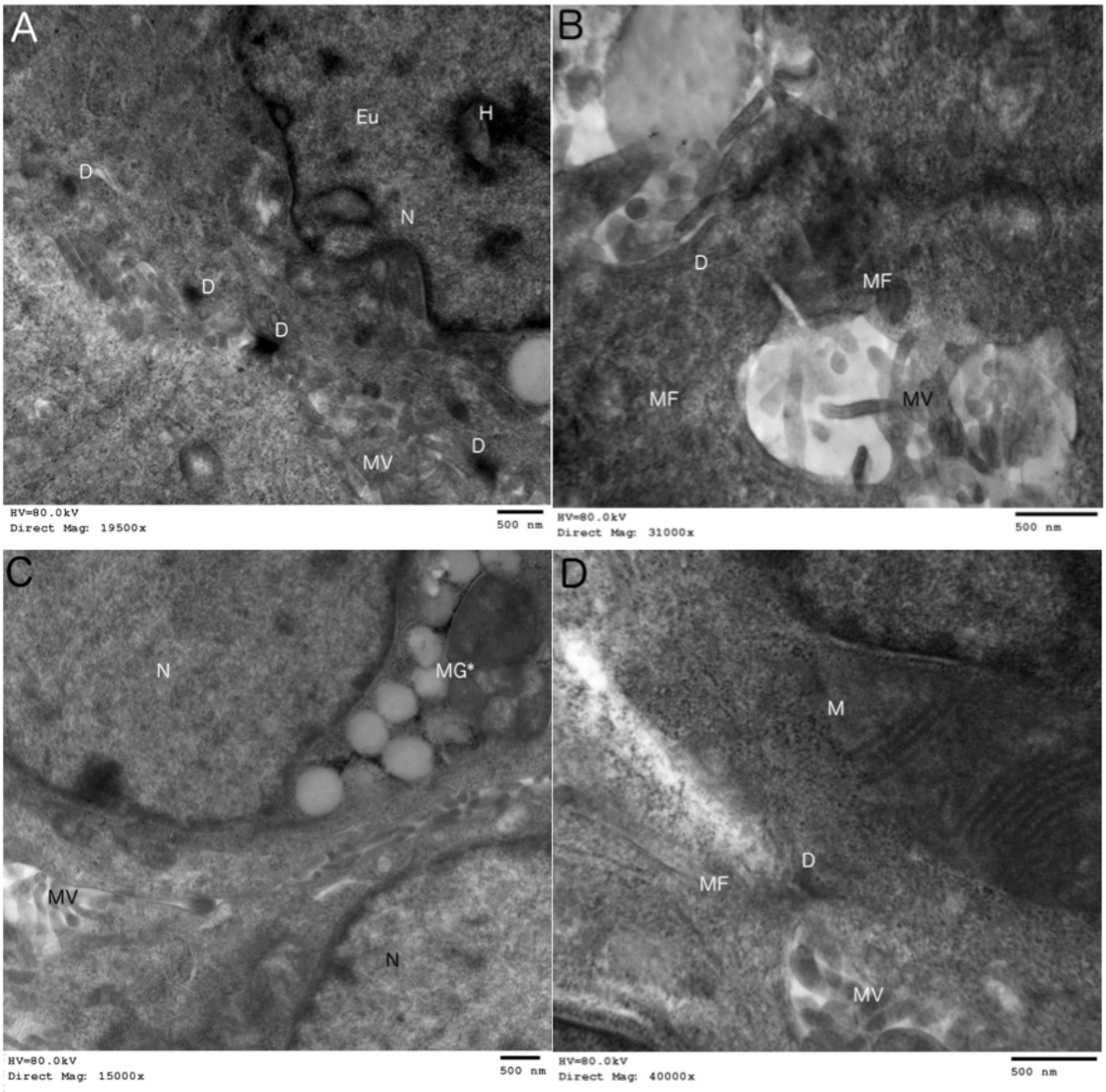

Figure 34. 5 mM NaBT treated HT29 micrographs. A- 29.9 x 10^3 magnification micrograph of a cell with four desmosomes at the cell-to-cell interface. Also some microvilli present between the two cells, as well as a well defined nucleus in the top left corner. B- 53.1 x 10^3 magnification micrograph of a desmosome and corresponding microfilaments. C- 25.7 x 10^3 magnification micrograph of what appears to be mucin granules near the nucleus. Dependent upon the orientation of the cell, this structure could also be part of the Golgi complex or vacuoles. D- 55.5 x 10^3 of a cell, mitochondria, desmosome, microfilaments and intracellular microvilli. (D: Desmosome, M: Mitochondria, MF: Microfilaments, MV: Microvilli, MG*: Mucin granules?, N: Nucleus)

REFERENCES

Abate-Shen, C., 2002. Deregulated homebox gene expression in cancer: Cause or consequence? *Nature Reviews Cancer* **2**:777-785.

Abdel-Fattah, R., A. Xiao, D. Bomgardner, C.S. Pease, M.B.S. Lopes, I.M. Hussaini, 2006. Differential expression of *HOX* genes in neoplastic and non-neoplastic human astrocytes. *Journal of Pathology* **209 (1):** 15-24.

Alcarraz-Vizán, G., J. Boren, W.N.P. Lee, M. Cascante, 2010. Histone deacetylase inhibition results in a common metabolic profile associated with HT29 differentiation. *Metabolomics* **6:** 229-237.

Amasheh, S., T. Schmidt, M. Mahn, P. Florian, J. Mankertz, S. Tavalali, A. Gitter, J.D. Schulzke, M. Fromm, 2005. Contribution of claudin-5 to barrier properties in tight junctions of epithelial cells. *Cell Tissue Res* **321**: 89-96.

Augeron, C., C.L. Laboisse, 1984. Emergence of Permanently Differentiated Cell Clones in a Human Colonic Cancer Cell Line in Culture after Treatment with Sodium Butyrate. *Cancer Research* **44**:3961-3969.

Barnard, J.A., G. Warwick, 1993. Butyrate Rapidly Induces Growth Inhibition and Differentiation in HT-29 Cells. *Gastroenterology* **4**: 495-501.

Barber, R.D., D.W. Harmer, R.A. Coleman, B.J. Clark, 2005. GAPDH as a housekeeping gene: analysis of GAPDH mRNA expression in a panel of 72 human tissues. *Physiol Genomics* **21**: 389-395.

Boudreau, N., C. Andrews, A. Srebrow, A. Ravanpay, D. Cheresh, 1997. Induction of the Angiogenic Phenotype by *Hox* D3. *The Journal of Cell Biology* **139** (1): 257-264.

Buccoliero, A.M., F. Castiglione, D. R. Degl'Innocenti, F. Ammanati, F. Giordano, M. Sanzo, F. Mussa, L. Genitori, G.L. Taddei, 2009. Hox-D Genes Expression in Pediatric Low-grade Gliomas: Real-time-PCR Study. *Cellular and Molecular Neurobiology* **29 (1):** 1-6.

Bustin, S.A., 2002. Quantification of mRNA using real-time reverse transcription PCR (RT-PCR): trends and problems. *Journal of Molecular Endocrinology* **29**: 23-39.

Candido, E. P. M., R. Reeves, J. R. Davie, 1978. Sodium Butyrate Inhibits Histone Deacetylation in Cultured Cells. *Cell* **14**: 105-113.

Chopra, D.P., A.A. Dombkowski, P.M. Stemmer, G.C. Parker, 2010. Intestinal Epithelial Cells In Vitro. *Stem Cells and Development* **19 (1):** 131-141.

Chen, F., M.R. Capecchi, 1999. Paralogous mouse *Hox* genes, *Hox*a9, *Hox*b9, and *Hox*d9, function together to control development of the mammary gland in response to pregnancy. *Proc. Natl. Acad. Sci.* **96**: 541-546.

Cohen, E., I. Ophir, Y. Ben Shaul, 1999. Induced differentiation in HT29, a human adenocarcinoma cell line. *Journal of Cell Science* **112**: 2657-2666.

Coradini, D., C. Pellizzaro, D. Marimpietri, G. Abolafio, M. G. Dadione, 2000. Sodium butyrate modulates cell cycle-related proteins in HT29 human colonic adenocarcinoma cells. *Cell Proliferation* **33**: 139-146.

Crosnier, C., D. Stamataki, J. Lewis, 2006. Organizing cell renewal in the intestine: stem cells, signals and combinatorial control. *Nature Reviews Genetics* **7**: 349-359.

Duenas-Gonzales, A., M. Candelaria, C. Perez-Plascencia, E. Perez-Cardenas, E. de la Cruz-Hernandez, L.A. Herrera, 2008. Valproic acid as epigenetic cancer drug: Preclinical, clinical and transcriptional effects on solid tumors. *Cancer Treatment Reviews* **34**: 206-222.

Eschrich, S., I. Yang, G. Bloom, K.Y. Kwong, D. Boulware, A. Cantor, D. Coppola, M. Kruhoffer, L. Aaltonen, T.F. Orntoft, J. Quackenbush, T.J. Yeatman, 2005. Molecular Staging for Survival Prediction of Colorectal Cancer Patients. *American Society of Clincial Oncology* **23** (15): 3526-3535.

Freschi, G., A. Taddei, P. Bechi, A. Faiella, M. Gulisano, C. Cillo, G. Bucciarelli, E. Boncinelli, 2005. Expression of *HOX* homebox genes in the adult human colonic mucosa (and colorectal cancer?). *International Journal of Molecular Medicine* **16**: 581-587.

Gamet, L., D. Daviaud, C. Denis-Pouxviel, C. Remesy, J.C. Murat, 1992. Effects of short-chain fatty acids on growth and differentiation of the human colon cancer cell line HT29. *Int J Cancer* **52:** 286-289.

"Gene Therapy for Cancer: Questions and Answers" National Cancer Institute, 2010. <http://http://www.cancer.gov/cancertopics/factsheet/Therapy/gene>

Godefroy, O., C. Huet, L.A.C. Blair, C. Sahuquillo-Merine, D. Louvard, 1988. Differentiation of a clone isolated form the HT29 cell line: polarized distribution of histocompatibility antigens (HLA) and of transferrin receptors. *Biology of the Cell* **63**: 41-55.

Gout, S., C. Marie, M. Laine, G. Tavernier, M.R. Block, M. Jacquier-Sarlin, 2004. Early enterocytic differentiation of HT29 cells: biochemical changes and strength increases of adherens junctions. *Experimental Cell Research* **299**: 498-510.

Greer, J. M., J. Puetz, K. R. Thomas, M. R. Capecchi, 2000. Maintenance of functional equivalence during paralogous Hox gene evolution. *Nature* **403**: 661-665.

Grier, D.G., A. Thompson, A. Kwasniewska, G.J. McGonigle, H.L. Halliday, T.R. Lappin, 2005. The pathophysiology of *Hox* genes and their role in cancer. *Journal of Pathology* **205**: 154-171.

Guo, R.J., E. Huang, T. Ezaki, N. Patel, K. Sinclair, J. Wu, P. Klein, E.R. Suh, J.P. Lynch, 2004. Cdx1 Inhibits Human Colon Cancer Cell Proliferation by Reducing B-Catenin/T-cell Factor Transcriptional Activity. *Journal of Biological Chemistry* **279**: 36865-36875.

Heerdt, B.G., M.A. Houston, L.H. Augenlicht, 1994. Potentiation by Specific Short-Chain Fatty Acids of Differentiation and Apoptosis in Human Colonic Carcinoma Cell Lines. *Cancer Research* **24**: 3288-3294.

Huet, C., C. Sahuquillo-Merino, E. Coudrier, D. Louvard, 1987. Absorptive and Mucus-secreting Subclones Isolated from a Multipotent Intestinal Cell Line (HT29) Provide New Models for Cell Polarity and Terminal Differentiation. *Journal of Cell Biology* **105**: 345-357.

Jones, P.A., S.B. Baylin, 2007. The Epigenomics of Cancer. *Cell* **128**: 683-692.

Khoa, N.D., M. Nakazawa, T. Hasunuma, T. Nakajima, H. Nakamura, T. Kobata, K. Nishioka, 2001. Potential Role of *HOXD9* in Synoviocyte Proliferation. *Arthritis & Rheumatism* **44 (5)**: 1013-1021.

Krishnaraju, K. B. Hoffman, D.A. Liebermann, 1997. Lineage-Specific Regulation of Hematopoesis by *Hox*-B8 (*HOX*-2.4): Inhibition of Granulocytic Differentiation and Potentiation of Monocytic Differentiation. *Blood* **90**: 1840-1849.

Kruh, J., 1982. Effects of sodium butyrate, a new pharmacological agent, on cells in culture. *Molecular and Cellular Biochemistry* **42**: 65-73.

Le Bivic, A., M. Hirn, H. Reggio, 1988. *HT29* cells are an in vitro model for the generation of cell polarity in epithelia during embryonic differentiation. *Proceedings of the National Academy of Science* **85**: 136-140.

Livak, K.J., T.D. Schmittgen, 2001. Analysis of Relative Gene Expression Data Using Real-Time Quantitative PCR and the $2^{-\Delta\Delta CT}$ Method. *Methods* **25**: 402-408.

Lorentz, O., I. Duluc, A. De Arcangelis, P. Simon-Assmann, M. Kedinger, JN. Freund, 1997. Key Role of the Cdx2 Homeobox Gene in Extracellular Matrix-mediated Intestinal Cell Differentiation. *The Journal of Cell Biology* **139**: 1553-1565.

O'Connell, J.B., M.A. Maggard, C.Y. Ko, 2004. Colon Cancer Survival Rates With the New American Joint Committee on Cancer Sixth Edition Staging. *Journal of the National Cancer Institute* **19**: 1420-1425.

Mankertz, J., J.S. Waller, B. Hillenbrand, S. Tavalali, P. Florian, T. Schoneberg, M. Fromm, J.D. Schulzke, 2002. Gene expression of the tight junction protein occluding includes differential splicing and alternative promoter usage. *Biochem and Biophys Res Comm* **298**: 657-666.

Macfarlane, S., G.T. Macfarlane, 2003. Regulation of short-chain fatty acid production. *Proceedings of the Nutrition Society* **62**: 67-72.

McCue, P.A., M.L. Gubler, M.I. Sherman, B.N. Cohen, 1984. Sodium Butyrate Induces Histone Hyperacetylation and Differentiation of Murine Embryonal Carcinoma Cells. *The Journal of Cell Biology* **98**: 602-608.

Pfaffl, 2001. Mathematical model for relative quantification in real-time RT-PCR. *Nucleic Acids Research* **29 (9)**: 2002-2007.

Privalsky, M.S., 1998. Depudecin makes a debut. *Proceedings of the National Academy of Sciences of the United States of America* **95 (7)**: 3335-3337.

Quintana, A.M., F. Liu, J.P. O'Rourke, S.A. Ness, 2011. Identification and Regulation of c-Myb Target Genes in MCF-7 Cells. *BMC Cancer* **11**: 30.

Ruijter, A.J.M, A.H. Van Gennip, H.N. Caron, S. Kemp, A.B.P. Van Kuilenburg, 2003. Histone deacetylases (HDACs): characterization of the classical HDAC family. *Biochemical Journal* **370**: 737-749.

Samuel, S., H. Naora, 2005. Homeobox gene expression in cancer: Insights from developmental regulation and deregulation. *European Journal of Cancer* **41**: 242-2437.

Schroy, P.C., A.K. Rustgi, E. Ikonomu, X.P. Liu, J. Polito, C. Andry, J. Connor O'Keane, 1994. Growth and Intestinal Differentiation Are Independently Regulated in HT29 Colon Cancer Cells. *Journal of Cellular Physiology* **161**: 111-123.

Shah, N., S. Sukumar, 2010. The *Hox* genes and their roles in oncogenesis. *Nature Reviews Cancer* **10**: 361-371.

Sjo, A., K.E. Magnusson, K.H. Peterson, 2003. Distinct Effects of Protein Kinase C on the Barrier Function at Different Developmental Stages. *Bioscience Reports* **23 (2,3)**: 87-102.

Tabuse, M., S. Ohta, Y. Ohashi, R. Fukaya, A. Misawa, K. Yoshida, T. Kawase, H. Saya, C. Thirant, H. Chneiweiss, Y. Matsuzaki, H. Okano, Y. Kawakami, M. Toda, 2011. Functional analysis of *HOXD9* in human gliomas and glioma cancer stem cells. *Molecular Cancer* **10**: 60.

Takahashi, Y., J. Hamada, K. Murakawa, M. Takada, M. Tada, I. Nogami, N. Hayashi, S. Nakamori, M. Monden, M. Miyamoto, H. Katoh, T. Moriuchi, 2004. Expression profiles of 39 *HOX* genes in normal adult organs and anaplastic thyroid cancer cell lines by quantitative real-time RT-PCR system. *Exp Cell Res* **293 (1):** 144-153.

Thompson, A., M.A. Rosenthal, S.L. Ellis, A.J. Friend, M.I. Zorbas, R.H. Whitehead, R.G. Ramsay, 1998. c-Myb Down-Regulation Is Associated with Human Colon Cell Differentiation, Apoptosis, and Decreased Bcl-2 Expression. *Cancer Research* **58**: 5168-5175.

Thornsteinsdottir, U., A. Mamo, E. Kroon, L. Jerome, J. Bijl, H.J. Lawrence, K. Humphries, G. Sauvageau, 2002. Overexpression of the myeloid-leukemia associated *Hox*a9 gene in bone marrow cells induces stem cell expansion. *Blood* **99**: 121-129.

Vandesompele, J., K. De Preter, F. Pattyn, B. Poppe, N. Van Roy, A. De Paepe, F. Speleman, 2002. Accurate normalization of real-time quantitative RT-PCR data by geometric averaging of multiple internal control genes. *Genome Biology* **3 (7)**: 1-12.

Van Wijk, R., L. Tichonicky, J. Kruh, 1981. The effect of sodium butyrate on the hepatoma cell cycle: possible use for cell synchronization. *In Vitro* **17 (10):** 859-862.

Vider, B., A. Zimber, D. Hirsch, D. Estlein, E. Chastre, S. Prevot, C. Gespach, A. Yaniv, A. Gazit, 1997. Human colorectal carcinogenesis is associated with deregulation of homeobox gene expression. *Biochemical and Biophysiological Research Communications* **232**: 742-748.

Ye, D.Z., K.H. Kaestner, 2009. Foxa1 and Foxa2 Control the Differentiation of Goblet and Enteroendocrine L- and D-cells in Mice. *Gastroenterology* **137**: 2052-2062.

Young, S.K., Tsao, D., B. Siddiqui, J.S. Whitehead, P. Arnstein, J. Bennet, J. Hicks, 1980. Effects of Sodium Butyrate and Dimethylsulfoxide on Biochemical Properties of Human Colon Cancer Cells. *Cancer* **45**: 1185-1192.

Yuan, J.S., A. Reed, F. Chen, C.N. Stewart, Jr., 2006. Statistical analysis of real-time PCR data. *BioMed Central Methodology* **7**: 85.

Zhu, P., E. Huber, F. Kiefer, M. Göttlicher, 2004. Specific and Redundant Functions of Histone Deacetylases in Regulation of Cell Cycle and Apoptosis. *Cell Cycle* **3 (10)**: 115-117.